International Journal of Minerals, Metallurgy and Materials
Accepted manuscript, https://doi.org/10.1007/s12613-026-3386-9

Self-supported Metal Aerogel Electrocatalysts for Oxygen Reduction Reaction: Opportunities and Challenges

Shaik Gouse Peera[1),*,✉], *Shaik Ashmath*[2),*], *Seung Won Kim*[1)], *Tae-Gwan Lee*[2)], *Myunghwan Byun*[3),✉] *and Chao Liu*[4),✉]

1) Natural Science Research Institute, College of Natural Sciences, Keimyung University, 1095 Dalgubeol-daero, Daegu 42601, Republic of Korea

2) Department of Environmental Engineering, Keimyung University, 1095 Dalgubeol-daero, Dalseo-gu, Daegu, 42601, Republic of Korea

3) Department of Advanced Materials Engineering, College of Engineering, Keimyung University, 1095 Dalgubeol-daero, Daegu 42601, Republic of Korea

4) Faculty of Materials Metallurgy and Chemistry, Jiangxi University of Science and Technology, Ganzhou, 341000, China

* These authors contributed equally to this work.

✉Corresponding authors:Shaik Gouse Peera E-mail: gouse@kmu.ac.kr; Myunghwan Byun E-mail:myunghbyun@kmu.ac.kr; Chao Liu E-mail:liuchao198967@126.com

Abstract

Development of highly activity, stable electrocatalysts for oxygen reduction reactions (ORR) remains a challenging task to improve the efficiency of fuel cells. Though the Pt and Pt-transition metal alloy-based catalysts stand out as the practical choice, still these catalysts suffer from the poor Pt utilization and stability. In this regard, highly electrical conducting, purely metallic, hierarchical 3D-porous and nanowire morphologies of metal aerogels as self-supported electrocatalysts have been gaining particular interest in the recent decade. Integrating unique features of metallic nature and porous nature of aerogels, metal aerogels are highly regarded as efficient catalytic materials, especially for electrocatalysis. In this review, we elaborate the overview of recent progress on metal aerogel catalysts for ORR. Metal aerogel catalysts are found to have excellent ORR activity due to their high intrinsic activity arising from excellent Pt utilization and exposure of active sites due to entirely metallic nature. Due to high Pt utilization several noble metal aerogel catalysts are found to exhibit higher mass activity than the traditional Pt/C catalyst and mass activity target of 440 A/g_{Pt} at 0.9 V vs RHE by DOE) 2025, suggesting the high potential of metal aerogels as ORR catalysts in fuel cells. Here, we summarize the recent and benchmark research outcomes of metal aerogel catalysts for ORR, their effects on the microstructural analysis on the catalyst layers, fuel cell performance and the cutting-edge modifications of the metal aerogel catalysts that are recently reported in the literature. We systematically reviewed the various aspects of metal aerogel catalysts synthesis, their advantages over traditional Pt/C catalysts, ORR kinetics and finally provided with future research directions and recommendations to further improve and integrate the metal aerogel catalyst into the realistic fuel cells.

Keywords: Oxygen Reduction Reaction, Electrocatalysts, Self-supported catalysts, Metal

aerogels, Mass activity

Introduction

Energy serves as the fundamental catalyst for productive endeavors, constituting the essential basis of a nation's economic and social activities [1,2]. Depleting fossil fuel abundance alarms the industrial sectors to look for alternative energy sources, for energy supply and reduction of environmental pollution. Emission of pollutants from fossil fuel-based energy materials including carbon monoxide, nitrogen oxides, hydrocarbons, and soot particulate matter from carbon-based fuels adversely affecting the environment and human health. Therefore, the research is focused on development of renewable fuel such as H_2 by overall water splitting, electrochemical, photochemical CO_2 reduction and renewable energy sources [3-5]. In this regard, PEM (polymer electrolyte membrane) fuel cells are attracting considerable attention due to their efficiency and applications in automotive industry [6]. Fuel cell is an electrochemical device that converts chemical energy into electric energy with the help of hydrogen fuel and oxygen as the oxidant. Electricity generation from the fuel cells attains due to electrochemical reactions on the anodes and cathodes. The cathodic oxygen reduction reaction is kinetically sluggish due to the requirement of high over potential for the cleavage of O=O bond, thus requiring highly efficient platinum-based catalysts that account for high cost of fuel cells that hinders the commercialization [7]. In addition to the high cost of the platinum-based cathode catalysts, both the catalyst degradation and electrode instability are some of the drawbacks that hinders commercial applications of fuel cells [8]. Though there are several alternative transition metal-based catalysts that have been developed, they are yet to compete with Pt based catalysts in terms of practical power outputs. Therefore, at this moment, the Pt based catalysts still remain the only practical choice for fuel cell stacks that can be hosted on commercial FCVs (fuel cell vehicles) [9]. With continuous efforts by scientists to reduce the cost of the Pt catalyst by enhancing the Pt utilization to a level of 0.25 g_{Pt} kW^{-1} and a total quantity of Pt catalysts, at 30 g per stack, significantly increasing fuel cell stacking costs, exceeding long-term objectives of 5 g per vehicle [10]. By 2030, the US (department of energy) DOE expects fuel cell systems to cost $80/kW [11]. Accordingly, FCVs are generally considered luxury vehicles that can only be affordable to a fraction of the consumers. In order to make the fuel cells commercial, it is paramount to reduce the cost of Pt based catalysts that remains the top priority [12]. In the past decade, several efforts have been made to increase the ORR activity of the Pt based catalysts and proposed a wide range of Pt based catalysts systems such as Pt/C, Pt and Pt alloy/de-alloy, Pt-transition metal alloys, Pt-rare earth catalysts, shape controlled noble metal catalysts, nano frames, nanohorns of noble metals, single atom catalysts and self-supported metal-only aerogel catalysts [13-23]. Most of these catalysts are synthesized and evaluated for their ORR in half-cell conditions and found to exhibit excellent ORR activity with 15 □ 36 times higher electrocatalytic activity than the commercial Pt/C catalysts at low to ultra-low catalysts loadings [24]. Though these catalysts displayed remarkable ORR activities only a few of them are found to be in commercial use, this is presumably due to several challenges that exist in synthesis, scale up of the catalysts at gram/kg levels and lack of real fuel cell experimental data [25].

High Pt utilization requires high dispersion of nanosized or atomically dispersed Pt on the high

surface area supports, to achieve high surface area-to-volume ratio which improves the accessible surface Pt atoms to the reactants (electrochemical surface area; ECSA). High Pt utilization eventually improves the mass and specific activities. Further, improvements in the ORR activities can be achieved by crystal phase engineering of the Pt nanoparticles that can exposure most favorable crystallographic planes towards ORR. This leads to an increase in the exposure of unsaturated coordination sites and modified electronic structure of the Pt nanoparticles that could improve the O_2 binding and its subsequent reduction to H_2O. For instance, Pt nanoparticles with Pt (111) phase are experimentally found to be highly favorable for ORR kinetics compared to Pt (110) and Pt (100) facets [26]. In addition, morphologies of nanoparticles are also found to positively affect ORR activity. For instance, it was proven experimentally that metallic Pt in the form of Pt-wires exposes abundant surface facets than the traditional Pt nanoparticles supported on carbon, believed to be originated from high stresses, surface undercoordinated metallic sites [27]. In addition to engineering the Pt nanoparticles with specific facet exposure, alloying the Pt with transition metal atoms are found to be an excellent strategy to improve the O_2 reduction kinetics [28]. The electrocatalytic properties of a Pt-M (platinum-based alloy) catalyst are governed by both the comprehensive lattice strain and the lattice contractions, which in turn increase the ORR activity. The former causes surface atoms to be exposed, high-index facets to be high, and uncoordinated atomic sites to be uncoordinated, while the latter causes a downshift of the d-band and reduces the unoccupied projected electronic states [29-32].

The mechanism of ORR on cathode of fuel cells includes several steps

(a) adsorption of O_2 on the catalyst surface
(b) electron transfer from the catalyst surface to the adsorbed O_2
(c) Weaking of the O=O bond and bond breaking between the two O molecules
(d) Product water formation and desorption (acid electrolyte) / formation of OH^- and desorption (alkaline electrolyte)

The ORR in acidic electrolytes and alkaline electrolytes proceeds either a direct 4 electron reduction process to form H_2O / OH^- ions respectively or a 2+2 reduction process via formation of H_2O_2 or HO_2^- as reaction intermediate products [33, 34] The adsorption of O_2 on the electrode surface can occur either side-on configuration, also known as Yeager model, where two O atoms coordinate with the active metal or end-on configuration, also known as Pauling model, where only one oxygen atom coordinate with the metal atom perpendicularly [35]. The reaction mechanisms of ORR in acidic and alkaline electrolytes are given below.

ORR in acidic electrolytes

Direct 4 electron reduction: $O_2 + 4H^+ + 4e^- \rightarrow 4H_2O \quad E° = 1.229\,V$

In-direct (2+2) electron reduction: $O_2 + 2H^+ + 2e^- \rightarrow H_2O_2 \quad E° = 0.670\,V$

$H_2O_2 + 2H^+ + 2e^- \rightarrow 2H_2O \quad E° = 1.776\,V$

ORR in alkaline electrolytes

Direct 4 electron reduction: $O_2 + 2H_2O + 4e^- \rightarrow 4OH^- \; E° = 0.401\,V$

In-direct (2+2) electron reduction: $O_2 + H_2O + 2e^- \rightarrow HO_2^- \quad E° = -0.065\,V$

$$HO_2^- + H_2O + 2e^- \rightarrow 3OH^- \quad E° = 0.867\,V$$

$$2HO_2^- \leftrightarrow 2OH^- + O_2$$

The electrocatalytic ORR activity of the catalyst are generally assessed via rotating disk and rotating ring-disk electrode (RDE/RRDE) measurements. The key indicators derived from RDE/RRDE measurements via linear sweep voltammetry are onset potential (E_{onset}), half-wave potential ($E_{1/2}$), overpotential at a specific current density (η_j), diffusion-limiting current density (J_L), kinetic-limiting current density (J_K), the electron transferred number (n), Tafel slope, electrochemically active surface area, turnover frequency, mass activity, peroxide formation by RRDE, stability test can all be derived from the measurement of polarization curves [35,36-37].

Among several emerging catalysts, self-supporting metallic aerogels are especially attractive due to the fact that, compared to shape controlled and nano frames noble metal catalysts, the metal aerogel catalysts are easier to synthesize and have potential to scale up to meet the commercial demands. In addition, the metal aerogel catalysts have several other advantages compared to traditional Pt/C and other alloys catalysts, as shown below.

1. Mitigates support corrosion: It is well known that traditional carbon supports are prone to degradation under electrochemical conditions thus leading to detachment of Pt nanoparticles and deterioration of the electrocatalytic activity. Moreover, the degradation of carbon support resulting from electrochemical carbon corrosion decreases the electronic conductivity of the catalysts. In contrast, metal aerogels mitigate carbon corrosion since it's all metal only composition and network of metal-metal bonds enhance the electronic conductivity.

2. High surface area to volume ratio due to unique porous 3D network: Compared to traditional carbon supported catalysts in which Pt nanoparticles buried deeply inside the dead-end porous networks, that are not available for electrochemical reactions, the metal aerogels exhibit high accessibility to the electrochemical reactions due to definite exposure of the active sites. Furthermore, the synthesis of aerogels comprised of reduction of metallic precursors with the reducing agents in an aqueous solution, which generally requires no further heat treatment process, whereas catalysts made of ordered alloys and intermetallic alloys generally requires heat treatment of the alloys at high temperatures to attain the desired ordering of the metallic atoms that also carries a risk of sintering of alloys into larger nanoparticles.

Metal aerogels enjoy the intrinsic porous network that allows easier access to inner metallic active sites by allowing the passage of gaseous reactants that are generally not accessible in case of random alloys, intermetallic alloys and ordered alloy catalysts. This high accessibility enhances the specific and mass activity of the catalysts that are highly desirable for reducing the catalyst cost and the catalyst loadings in the membrane electrode assemblies (MEAs). In addition, the aerogel catalysts are mechanically stable due to conscious metallic bonds that are well connected to each other, unlike other catalyst morphologies.

3. Ease of synthesis: Aerogel catalysts are generally synthesized in a single step, compared to other catalysts synthesis schemes such as core-shell catalysts that require multiple steps with precise control of the core and shell morphology. In addition, the core-shell catalyst also suffers from the instability of the shell and strain relaxation of the shell over time and selective leaching

of the shell metallic active sites. In addition, extremely high ORR active catalysts such as nanocages or hollow morphological alloys synthesis requires extremely price control on growth kinetics and generally require templates to construct the frame morphology.

4. Robustness of the metal aerogel catalysts: Metal aerogel catalysts are believed to be robust due to continuous 3D network of the metallic sites and are resistant to the collapse of the 3D network during potential cycling or stability tests. Whereas the ORR catalyst made of nanocages or hollow morphological alloys are prone to collapse and are extremely difficult to scale up to the gram levels, despite their excellent mass and specific activities.

5. Thin catalyst layer in PEM fuel cells electrode: Un supported metal aerogel catalysts are particularly important in PEM fuel cells electrode configuration as they significantly reduce the catalyst layer thickness. For instance, considering a catalyst loading of 0.2 mg Pt cm^{-2} in an MEA configuration, with 50 wt% Pt, ionomer to carbon ratio of 1, the total catalyst layer thickness account for about 5 µm [38]. This catalyst layer thickness contributes from the carbon support. With a similar catalyst loading using un-supported metal aerogel catalysts could drastically reduce the catalyst thickness by 90% and account for a final catalyst layer thickness as low as just 0.5 µm. When appropriate porosities and pore size modulation, metal aerogel catalysts could potentially reduce the resistance to the transport of electrons, protons, reactants, and product water could be easier in self-supported catalysts. Figure. 1a show the roadmap of significant milestones achieved int the synthesis of metal aerogel catalysts since their first discovery in 2009 by Prof. Alexander Eychmüller research group. Figure. 1b shows the schematic representation of differences between carbon supported vs self-supported metal aerogel catalysts.

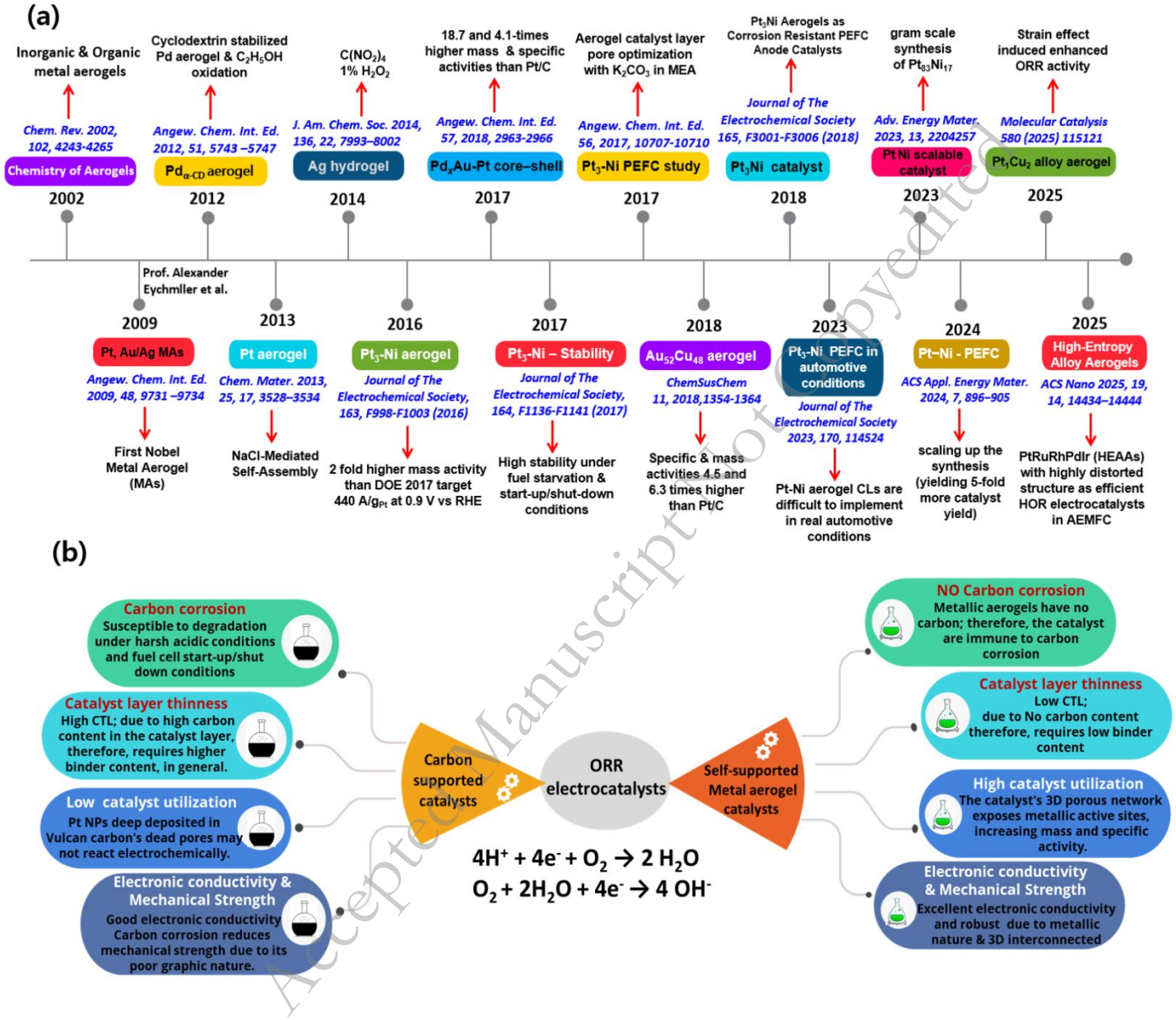

Figure 1. *(a) Timeline representing the significant milestones in the metal aerogel synthesis (b) schematic representation of differences between carbon supported vs self-supported metal aerogel catalysts.*

Among the unique features listed above, mitigating carbon support corrosion is considered as one of the important aspects of self-supporting metallic aerogels. Due to the absence of carbon support, the self-supporting metallic aerogels are potentially less susceptible to other degradation phenomena observed under normal PEM fuel cells operation, such as catalyst particle migration, dissolution and Ostwald ripening, due to their extended surface areas [39].

Carbon support corrosion is considered as a major factor for the degradation of catalyst especially at the high potential conditions (> 1.40 V) that exist during start-up and shut-down process [40]. Support stability is a major issue despite the fact that graphitized carbon supports including graphene, carbon nanotubes, and carbon nanofibers have been developed to lessen carbon corrosion. [41]. In this regard, aerogels and metal aerogels are advantageous for electrocatalysis due to their huge surface area, high porosity mechanical stability, and long metallic backbones [42,43]. The porosity of the catalyst and catalysts support is very important to transport the gaseous reactants to the catalyst surface and hence reduces the mass transport resistance in the catalyst layer and carbon-based gas diffusion layers factors such as such as pore shape, surface area, and pore volume are the important features [44]. The development of non-carbon support or supportless catalysts can be two possible alternatives for eliminating the carbon support from the electrocatalysts. There are efforts made to development non carbon supports such as TiO_2, SnO_2, Nb-doped SnO_2, WO_3, In_2O_3, ZrO_2, Ta_2O_5, SiO_2, and CeO_2 catalysts [45]. Among them, CeO_2 based catalysts have been intensively studied due to their excellent redox properties as electrocatalyst and catalyst supports [46,47]. However, none of the catalysts have been successfully implemented in the real, commercial fuel cell stacks, due to poor performance especially related to their insufficient surface area and electronic conductivity. The other best alternative is to develop electrocatalysts that are completely devoid of carbon support by developing all-metallic aerogel catalyst that can eliminate the need for carbon support and essentially mitigates carbon corrosion and their associated catalysts degradation phenomenon such as catalyst particle migration, dissolution and Ostwald ripening, due to their extended surface areas [48]. In addition, being all-metallic they exhibit excellent electronic conductivity. Therefore, metallic aerogels could be considered as the best alternative to the traditional carbon supported catalysts.

In this review, we overviewed the potential of metal aerogel catalysts in cathodic ORR electrocatalysis especially focusing on the PEM fuel cells. A brief introduction to the aerogels, synthesis strategies and characteristics of aerogel catalysts, followed by a deeper understanding of ORR activities and factors responsible for enhanced mass and specific activities of the catalysts will be discussed, finally future research directions and perspectives will be conferred. In recent years, there have been number of review articles on ORR electrocatalysts especially focusing on non-precious metal electrocatalysts mainly composed of transition metal catalysts such as Co, Fe, Mn, Cu and Ni in combination with N-doped carbon that potentially form M-N-C (M=TM) catalysts [49-52]. Metal-organic framework (MOF) derived M-N-C catalysts have been so far very popular for ORR and other electrochemical reactions [53,54]. It is generally known that M-N-C catalysts exhibit ORR activity similar to Pt/C, and because they are composed of earth-abundant metals, they lower the cost of electrocatalysts. There are number of electrocatalysts that exhibited excellent ORR activity. However, there exists number of limitations for non-precious, transition metal-based M-N-C catalysts such as their lower ORR activity in acidic electrolytes, lower stability under long term durability tests, their inability to catalyze a direct 4 electron reduction of oxygen especially Fe-based catalysts that produce considerable amount of H_2O_2, hydroperoxide (HO_2^-) ions in acidic and alkaline ORR, respectively [55]. In addition, at present the non-precious metal catalysts are still at R&D levels [56]. Therefore, the Pt based catalysts are still considered the only practical choice for fuel cells

at present and therefore, the Pt based catalyst research still continues to produce high quality research outputs [57, 58]. In this regard, there are number of Pt-alloy based research and review articles that have been published in recent times [59-60]. However, review articles on metal-aerogel catalysts are rare. The existing reviews on metal aerogels mostly summarize the noble metal aerogels synthesis, characterization, and application as electrocatalysts for general applications [61, 62]. However, the recent advances and critical analysis on the application and practical implications of the metal aerogels especially focusing on the fuel cell applications, to the best of our knowledge are scarce. Therefore, in this article we present recent advances and applications of metal-aerogels for ORR focusing on fuel cell applications have been overview and summarized.

What are metal aerogel catalysts and how they are made?

Aerogels are the synthetic solid materials that possess ultralow density, highly interconnected porosity together with high surface area, obtained from the self-assembly of colloidal noble metal nanoparticles. Metal aerogels are in general obtained *via* the sol-gel, galvanic replacement reaction (GRR), underpotential deposition (UPD) techniques, among them sol-gel synthesis process is generally considered as the most popular one that consists of three steps (i) obtaining the colloidal metallic nanoparticles (ii) formation of hydrogel from the colloidal metallic nanoparticles via destabilization/gelation (iii) obtaining the aerogel by supercritical drying of the hydrogel [63]. The metallic colloidal nanoparticles are made from metal precursors, a reducing agent (ex. $NaBH_4$ etc) and a stabilizer (ex. citrate and cyclodextrin *etc*) [64]. The use of stabilizers are generally essential to control the size and distribution of metallic nanoparticles. The subsequent gelation stage, which may be achieved by a spontaneous gelation process, relies on the stabilizers' and metal NPs' very weak coordination interaction between them. Gelation process is generally achieved by a spontaneous aging of the solution [65] or by adding destabilizers such as salts [66] cross linkers [67] or by applying physical agents such as heating [68]. During the gelation process colloidal spherical metal nanoparticles transform into highly interconnected 3D continuous network of nanowires which are transformed into porous aerogels *via* supercritical drying. The drying of the hydrogel involves eliminating the solvent from the interstitial positions in the metal hydrogels, which must be performed by a specialized drying technique called supercritical drying which preserves the porous, interconnected network into the aerogel that is inherited from the hydrogel. In contrast, removing or getting rid of the solvent by a simple thermally- mediated (or -driven) evaporation leads to collapse or shrinkage of the porous network that exists in the hydrogel due to high surface tension or capillary pressure. The supercritical dried hydrogels result in aerogels with excellent surface area and porosity and extremely low density that can be used for electrocatalytic applications. The metallic aerogel nanoparticles of various precious metals such as Pt, Pd, Au, Ag, Cu, PtPd, PdAu, PtCu *etc* have been already obtained and found to exhibit excellent 3D porosity ranging from micro to meso- and macroscale pores with a uniform size distribution [69].

Metal aerogels are synthesized *via* two pathways (i) Two step-scheme or (ii) one step-scheme based on whether or not the colloidal nanoparticles are separated before the gelation [Figure. 2a-c]

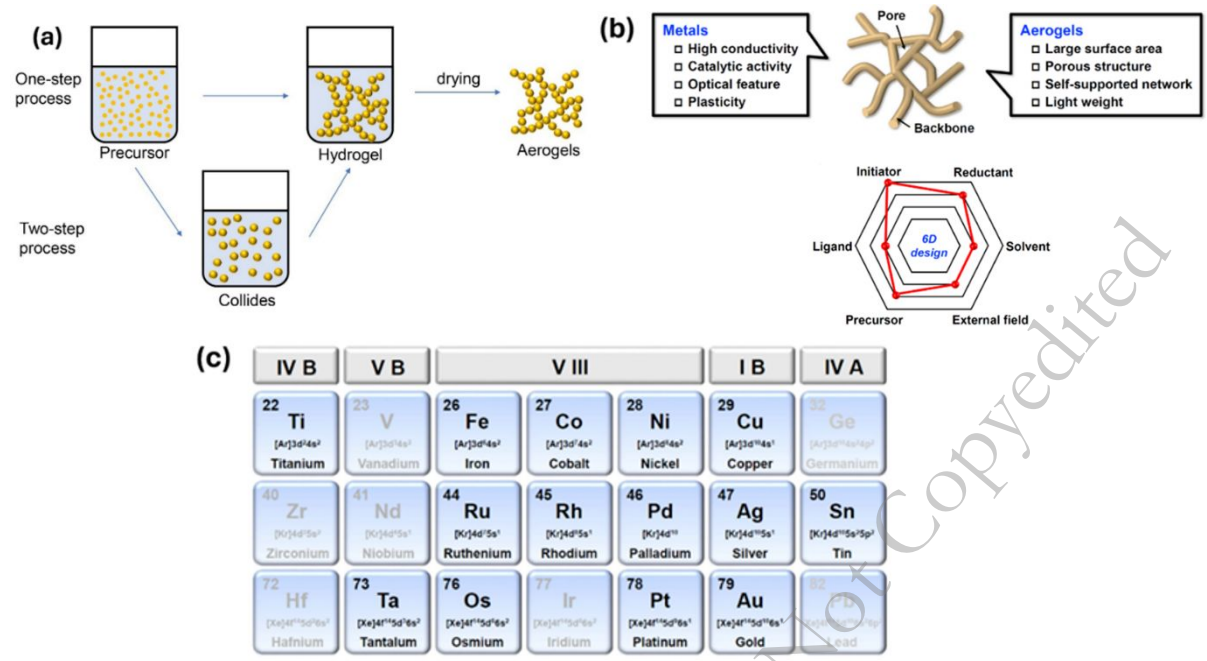

Figure 2. *Schematic representation of (a) one and two step metal aerogel synthesis [Reproduced from Ref. 64, open access] (b) metals that are successfully synthesized as metal aerogels (c) metal and aerogel properties of metal aerogels and 6D representations of factors that affect the metal aerogel synthesis [Reproduced with permissions from Ref. 95]*

Two step-schemes: The colloidal nanoparticles are synthesized followed by purification/concentration and gelation. Most of the metal aerogels synthesized are results in nanowire morphology, irrespective of the two step or one step synthesis route. Two step method is the first of kind reported for the synthesis of Au, Ag, Pt, Ag-Au and Pt-Ag metal aerogels which is traced back to 2009. In a typical synthesis, a citrate stabilized nanoparticle solution is obtained from the $NaBH_4$ reduction of metal precursors, was concentrated by ultracentrifugation to obtain a final concentration of 10 mM, the hydrogels are obtained in about 1-4 weeks. Such long gelation time significantly lengthens the synthesis process. To reduce gelation time and quicken the gelation kinetics, several synthesis medications have been investigated such as increasing the temperature, adding gelation initiators such as salts, dopamine, N_2H_4 [70,71].

***One step-scheme*:** The nanoparticles formation and gelation are combined, meaning the gelation occurs spontaneously during the reduction of metal precursors *via* reducing agents without any additional agents to accelerate the gelation kinetics such as salt. The first research report on one step scheme was published in 2012 by Liu et al [65, 72] by using cyclodextrin stabilized Pd aerogels with $NaBH_4$ as reducing agent. Followed by this, a number of researchers reported that several single metal aerogels or dual metal alloy aerogels have been developed such as M-Cu (M-Pd, Pt and Au) with the gelation time of about 6 h via increasing the reaction temperature. The most common reducing agent used both in two-step and one-step scheme is $NaBH_4$, other reducing agents used are ascorbic acid, NaH_2PO_2 were also explored. The metal

aerogels of a single metal, bimetallic or multiple metals can be synthesized by carefully selecting the precursors and choosing a suitable reductant reaction condition and the gelation methods to obtain the single, bi or multimodally aerogels [73].

Metal aerogels possess mixed functions from the metals and aerogels, that include high electronic conductivity, catalytic activity, large surface area, porous structure, light weight, self-supported networks and plasticity. The synthesis of the metal aerogels depends on six important factors such as (1) gelation initiators, (2) precursors, (3) reductant, (4) solvent, (5) external field, (6) ligand.

1. Gelation Initiators: Initiators are the important component that determines the formation of gel and assist in gelation, which are broadly classified into chemically induced or thermally induced initiations. The gel formation by the destabilization of the Au NPs by pH (11.9 – 12.4) was the first proposed strategy to obtain the monolith metal gel in the presence of D-glucose [74]. Later, H_2O_2 mediated fusing of the naked nanoparticles have been produced by Eychmuller's research group for the first time in 2009 opened a new avenue in the field of metal aerogel synthesis process [66]. First, the naked metal nanoparticles are prepared by $NaBH_4$ reduction method in the presence of stabilizer ligand, which was then etched by the oxidant that yields the metallic hydrogel, upon sequential solvent exchange and supercritical drying gives a metal aerogel of various sizes ranging from 100-500 nm for Au, Ag and for alloys the metal nanoparticles size has been reduced to around 10 nm. However, the hydrogel formation time was time consuming, lasting about 1–4 weeks. In order to reduce the gelation time, tetranitromethane mediated strategy was developed for Ag nano-shell metal aerogel in which the gelation time was brought to significantly lower time with just 4 -12 h [75]. Another notable work was performed by Liu et al [65,72] where a reductant-based gelation process was achieved by adding small of amount of reductant to the dilute solution of mean salts that induce the formation of metallic nanoparticles as well as promoting the gelation of noble metals such as Pd and Pt-Pd gels, in a single step synthesis process. In another study, dopamine was used as the chemical agent to induce the gelation of Au gel [76]. In contrast to previous methods, dopamine mediated gelation yields the smallest Au nanoparticle size of about 5-6 nm, whereas other methods yield nanoparticles of around 100 nm range. In addition to organic ligands as initiators, several IA and IIA metal ions such as Ca^{2+}, Mg^{2+}, Na^{+} and K^{+} have been utilized [77-79]. Physical and chemical initiators, several physical agents have been known to induce the initiation of the gelation process such as, concentrating the nanoparticles solution by simple evaporation [80,81] by freeze-casting [82,83] or freeze thaw methods [84].

2. Precursor: The precursors used to synthesize the metal aerogels are broadly classified as metal salts metal building blocks such as nanoparticles and nanowires and metal gels. Among these using simple (i) metals salts such as metal nitrates, metal chlorides, metal sulphides and metal acetates are some of the examples. Use of simple metal salts is the simple synthesis process, ease of availability and cost effectiveness. However, the influence of each type of salt has not been investigated. In addition, use of simple salts and reducing them to metallic state is always accompanied by uncontrolled morphology and growth [65]. In contrast, using (ii) metal building blocks assists in controlling the metal nanoparticle morphology and growth due to twostep process comprising synthesis and assembly in two distinct steps. In general, the use of metal building blocks synthesis strategies requires capping agents/stabilizing agents which act as ligands or organic solvents like 1-octadecene to stabilize the colloidal nanoparticles [66,

68, 85]. Though the use of capping agents or organic solvents benefits controlling the nanoparticle size and morphology, usually they are associated with issues such as complicated synthesis process, requiring specific ligands contributing to the high cost of the catalysts system, in addition to the difficulty in removing the ligands completely from the nanoparticles surface. On the other hand (iii) using previously formed gels as precursors offers an excellent opportunity to tine the inter-connectivity and morphological and compositional properties of the metal aerogels. In this case, GRR is a very frequently employed technique. For example, Metallic Pt atoms are deposited on the previously formed Pt-Ag gel by Ag in the presence of Pt ions, which results in enhanced specific surface area of around 8 times [86]. Similarly, PdAu-Pt core-shell nano aerogels were also performed on the Pd-Au hydrogel [87]. In another study, a post treatment process was followed to insert shell metal atoms on the previously formed core metal atoms by adding shell metal ions to the undergoing generation of core metal gels. Simply during generation of the core metal, the salts for the shell metal were added to form a core shell 3D metal aerogel [77]. Though using gels as precautions provides tremendous opportunities to tune the composition morphology of the metal aerogel materials, these processes involve multiple steps time consuming, complicating the whole synthesis process and sometimes cannot guarantee the desired properties to the metal aerogels. Among three types of metal precursors metal salts results in high reproducibility in terms of synthesis than the other type of precursors.

In short conclusion, it is very crucial to choose the metal precursors for obtaining metal aerogels of desired properties. In almost all reports the use of metal saws as precursors is a common protocol due to ease of obtaining metal precursors and simple handling of the entire synthesis process.

3. Reductants: Use of reductants seems to be mandatory to convert ionic metal precursors into zero valent metallic atoms. The most used reductant is sodium borohydride ($NaBH_4$), though there are other reductants such as hydrazine, dimethylamine borane, and Na_2HPO_2 have also been explored. When using sodium borohydride, it is of importance to note that reductant to metal ratio (R/M) is an important factor to obtain the metal aerogels, which is roughly 4:0. It is worthy to note that smaller than ratio 4 also works well to reduce the metallic ions into gels however the lowest reductant ratio ($R/M < 2$) in the absence of any stabilizers would lead to spontaneous aggregation of the formed metal atoms into agglomerated nanoparticles rather than the desired uniform sized nanoparticles [88]. Unreacted $NaBH_4$ molecules stabilize the NPs at medium R/M ($2 < R/M < 50$), creating a sable NP sol, in addition to acting as a reductant due to the high affinity between BH_4^- and Au. Initiators are activated at even higher R/M values ($R/M > 50$), when a flood of ions released during the dissociation of $NaBH_4$ causes the in situ formed NPs to gel via the salting-out effect. The observed phenomena were explained clearly by the R/M-dependent triple functions of the reductants, which were revealed in this light. On the other hand, when the $R/M > 100$, the extremely excess reductant concentration is found to have an unbelievable stabilizing effect on nanoparticles. Therefore, the type and concentration of the product is found to have significant effect on the size of the nanoparticles and the stabilization effects.

4. Use of ligands: Use of organic ligands, and polymers is well documented in the nanoparticle's synthesis due to their specific interactions with the metal nanoparticles in tailoring the particle size distribution, facet engineering, controlling the shape and morphology

of metal nanoparticles. However, the use of ligand also draws criticism, due to shielding effect and inability to be taken out completely from the surface. Therefore, the use of ligands and their chemistry of interaction needs to be understood clearly. Several other alternatives have been explored, such as CO gas, and certain types of electrolytic salts such as trisodium citrate have shown considerably positive effect as stabilizers for nanoparticles and promote gelation [89].

5. Solvents: Solvents play an important role in dispersing the metal precursors and establishing polar or non-polar interactions with the ligands and nanoparticles. While the use of solvents also contributes to the cost of the catalyst synthesis, the use of green solvents eases the entire process. H_2O is the most utilized solvent in the synthesis process. The use of non-polar solvents such as carboxylic-acid-based solvents, 1-octadecene, and hexane have been explored only since 2016 [85, 90]. In addition to the role of solvents as dispersing agents, the addition of external miscible solvents such as ethanol to the water is found to destabilize the nanoparticles and hence initiates the gelation [66] Other miscible and immiscible solvents systems such as ethanol, ethanol/toluene have also been employed [91,92].

6. Effect of external fields: In addition to reaction system ingredients, external factors can significantly impact the gelation process and resulting MAs. Investigations have focused on the effect of temperature (313–348 K). Gelation kinetics have been found to be positively affected by the increased reaction temperature [93,94]. For Instance, the gelation time was significantly reduced to 12h from 2-3 weeks by employing the temperature of 348K [68]. On the other hand, reducing the reaction temperature to freezing levels also enhances the gelation. In a study, it was found that reducing the reaction temperature to freezing gels reduces the solation ability and enlarges the volume. Consequently, the solutes are extricated from the aqueous phase and directed to the interfaces of ice crystals, thereby forming three-dimensional networks facilitated by the ice templates and resulting in self-supported aerogels post-sublimation. However, freeze-casting may not be suitable if the ligands are used to cap the nanoparticles as they contaminate the aerogels during the freeze-drying.

In short summary, the choice of synthesis components determines the final structure, morphology, specific surface area, and electrocatalytic properties of the metal aerogels. The very important stage of metal aerogels synthesis is the gelation step, which requires careful manipulation and attention during the synthesis [95].

Metal aerogels as electrocatalysts for ORR

Most of the basic research work on the electrocatalysis of the self-supported metal aerogel catalysts was performed by Alexander Eychmuller research group at the department of Physical Chemistry, Technische Universitat Dresden, Germany and that work still remains the classical bench marking research on basic understanding of metal aerogel electrocatalysis. The first noble metal-based aerogel catalysts was synthesized by Alexander et al back in 2009 [66] with a surface area of 48 $m^2\ g^{-1}$ for Ag/Au and 46 $m^2\ g^{-1}$ for Pt/Ag. The synthesis process was later extended to Pd aerogel catalysts by using cyclodextrins as a stabilizer and $NaBH_4$ as reductant, the obtained self-supported Pd aerogel catalysts were applied for ethanol electrooxidation, this opening the new avenue in the aerogel application in the electrocatalysis [72]. The Pd_{CD} metal aerogel shown to have highly porous, interconnected networks of Pd in the form of nanowires of a diameter of 3.6 nm. The nanowires of Pd_{CD} networks are further fused and interconnected

to form a highly branched structure. The XPS analysis shows the Pd atoms are entirely made of zero valent metallic state, with an enhanced surface area of 92 $m^2 g^{-1}$, almost the double the surface area of their previous work suggesting that manipulating the synthesis process, gelation and stabilizers can enhance the porous network and surface area of the resulting metal aerogels. The resulting Pd_{CD} metal aerogel catalysts exhibited enhanced oxidation current for ethanol than the commercial Pd/C catalysts. Inspired from the above, Alexander et al extended the knowledge of noble metal aerogel to incorporate non-noble metal into the noble metal aerogel resulting in the synthesis of Pt-Ni aerogel that resulted in a 2-fold enhanced ORR activity [**96**]. In a typical synthesis, aqueous solution of metal precursors was reduced by aqueous $NaBH_4$ solution that reduced the ionic Pt^{4+} and Ni^{2+} ions into a metallic state resulting in the Pt-Ni aerogel. The reduction of the metallic ions can be clearly seen when the color of the solution turns black from light yellow. The resulting solution was then allowed to settle down to the bottom of the vial to form the hydrogel, which was later dried in a supercritical CO_2. The TEM measurements revealed no isolated particles of PtNi, instead the PtNi nanoparticles fused and interconnected to form a highly porous 3D metallic network. Moreover, the morphology of the PtNi aerogels were found to be highly reproducible, demonstrated by the batch scale synthesis. The XRD analysis of the PtNi aerogel clearly revealed formation of alloy represented by shift in the 2theta of the peaks related to Pt. The synthesized Pt_3Ni and $Pt_{1.5}Ni$ reach the DoE ORR and mass activity target at 0.95 V vs RHE that was extrapolated from the reported value of 440 A/g_{Pt} at 0.9 V vs RHE ≈2-fold higher than Pt/C catalyst [Figure. 3a-c]. In a continuous study, authors applied the self-supported Pt_3Ni in the fuel cell cathodes and studied the PEFC performance [**97**]. The H_2/air fuel cell performance of the Pt_3Ni aerogel revealed a significantly lower performance than the Pt/C catalyst, due to larger mass transport losses, though the RDE results showed 3 times higher performance. The lower performance of the Pt_3Ni is attributed to the concentrated mesopores in the catalyst layer which are believed to be less effective in transporting the gaseous reactants. To improve the porosity, K_2CO_3 salt is added during the ink preparation, since the salt can be easily removed from the catalyst later by simple washing, in addition, the ability to evolve CO_2, that can enhance the catalyst layers porosity. The catalyst ink was carefully optimized with salt + nafion content + catalyst ratio via RDE studies and the optimized proportions are then coated by catalyst coated membrane (CCM) method for fuel cell testing. The improved version of Pt_3Ni aerogel in the fuel cell testing exhibited remarkable performance, especially in the mass transport region, resulting in higher power density. The improved Pt_3Ni aerogel shows 2.5-fold higher specific activities. This work has motivated us to further explore the self-supported metal aerogel catalysts for ORR activity.

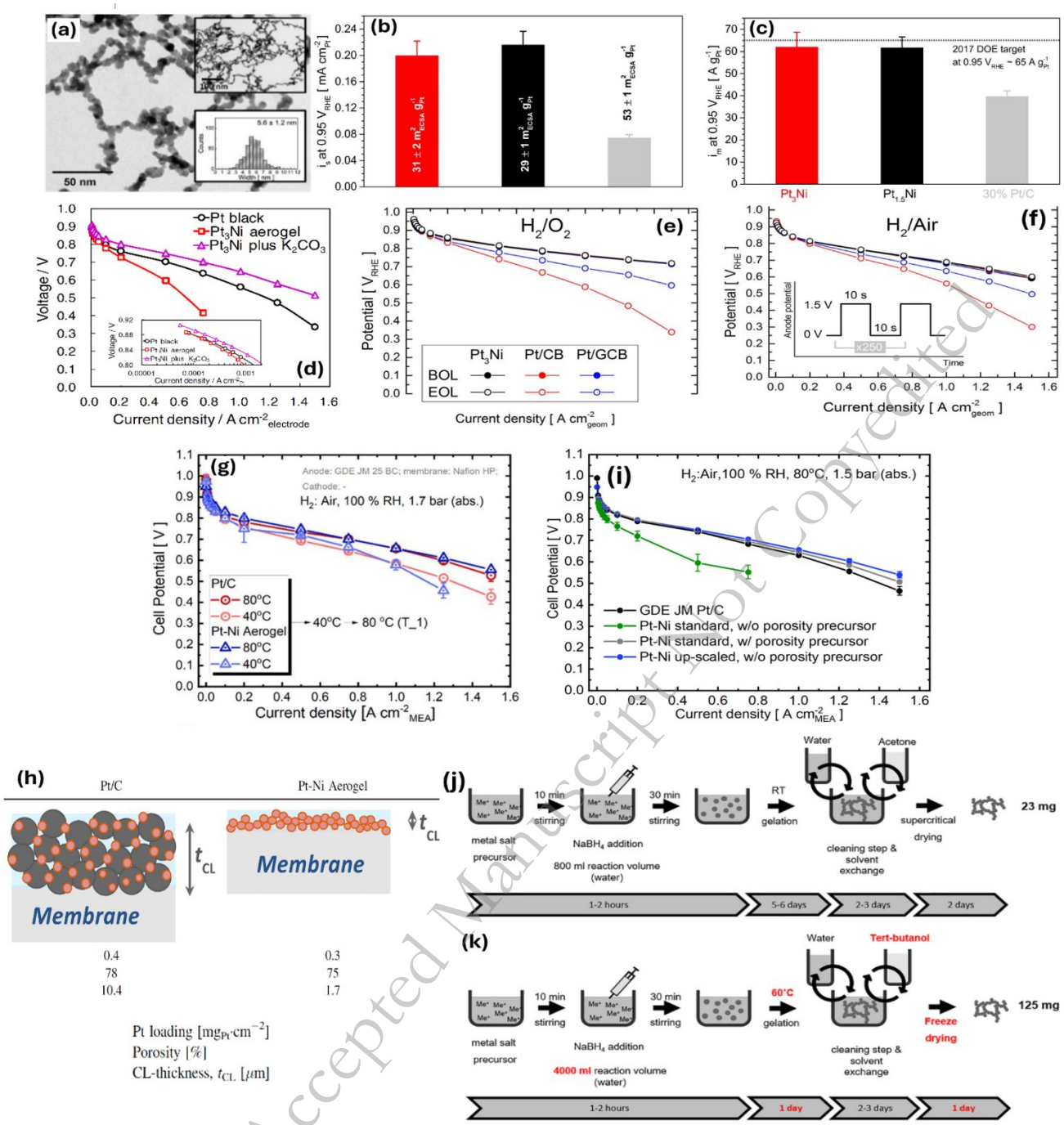

Figure 3. *(a) TEM image of the Pt_3Ni catalyst (b, c) ECSA, mass specific activity of Pt-Ni aerogel and Pt/C catalyst at 0.95 V [Reproduced from Ref. [96] open access]. (d) i-V curves and Tafel plots of the Pt black, Pt_3Ni aerogel, Pt_3Ni plus K_2CO_3, corresponding MEAs [Reproduced from Ref. [100] open access]. (e,f) BOL and EOL of i-V a Pt_3Ni aerogel, Pt/CB and Pt/GCB MEAs in H_2/O_2 and H_2/Air conditions, respectively [Reproduced from Ref. [103], open access] (g) i-V curves of Pt/C and Pt-Ni aerogel (h) Graphical representation of the benchmark Pt/C and Pt-Ni aerogel CLs, along with their corresponding porosities and thicknesses [Reproduced from Ref. [105] open access]. (i) i-v curves of Pt-Ni aerogel in standard and upscaled process (j,k) schematic showing the upscaled synthesis process for PtNi aerogel catalyst [Reproduced with permissions from Ref. 106].*

In another study, Henning et al [98] investigated the durability of Pt_3-Ni aerogel in PEFC cathodes. It is well known that durability of the PEFCs is one of the concerns in terms of commercial applications, especially the cathode Pt/C catalysts stability. Corrosion of carbon support under highly acidic and oxidative environment, high cathodic potential (> 1.2 V) accelerates the electrochemical carbon corrosion that leads to Pt nanoparticles agglomerations and detachment from the surface leads to decreased ORR activity. Since self-supported metal aerogel catalysts are composed entirely of metal rather than carbon, they should, in theory, be more durable than supported catalysts. This is one of the many advantages of self-supported metal aerogel catalysts. Aiming at this the authors investigated previously synthesized Pt_3-Ni metal aerogel catalysts durability following DoE protocols with two different accelerated stress tests (ASTs). The first AST focus on the mimicking the "start-up/shut-down" conditions of the fuel cells un the potential region of 1.0 to 1.5 V vs RHE and other ASR focus on the normal operating power output conditions of fuel cells in the potential range of 0.6 – 1.0 V vs RHE, which potentially causes the Pt dissolution and re-deposition, denoting as "load-cycle degradation". Surprisingly, Pt_3-Ni aerogel catalysts exhibited excellent stability in both the ASTs when compared to Pt/C. In the start-up/shut-down test of 10,000 potential cycles Pt_3-Ni catalyst show only a marginal decrease in mass and specific activities, ECSA from the beginning of the life test (BOL), whereas Pt/C catalyst showed almost a reduction of 50% in mass and specific activities at the end of the life (EOL) test. This is also translated into the H_2/air polarization curves in which Pt_3Ni catalyst shows a similar I-V curves BOL and EOL, whereas a drastic performance loss has been observed for Pt/C catalyst. Authors also compared the Pt_3Ni superiority over Pt/graphitized carbon catalysts, where a 50% reduction in the MA and ECSA was observed for Pt/ graphitized carbon catalysts. Under the "load-cycle degradation" AST, both Pt/C and Pt_3Ni showed a similar degree of performance reduction in MA and ESCA. While probing the reason behind the degradation, it was found that the microstructure and porosity of Pt_3Ni catalyst show similar morphological observations before and after the end life test, whereas Pt/C catalyst showed a compact and less porous (compact) morphology, that resulted in increased mass transport resistance for gaseous oxygen in the air and hence reduces the performance. Further, morphological observations from the TEM show consisted of well-defined 3D network of interconnected Pt_3Ni nanoparticles, whereas the Pt/C catalyst showed carbon support corrosion during start-stop degradation, becoming more and more amorphous leading to decreased fuel cell performance.

One of the important aspects of realistic fuel cells is the diffusion of O_2 towards the catalyst surface which increases mass transport resistance that directly influences the fuel cell performance, especially when using air as oxidant. The O_2 diffusion occurs due to O_2 gradient in the catalyst layer. When using Pt/C as catalyst which accounts for 10 -20 μm catalyst layer thickness (considering a catalyst loading of 0.4 mg_{Pt}/cm^2), the self-supported catalyst typically attains a 10 times lower catalyst layer thickness of 1-2 μm, significantly reduces the catalyst layer thickness which negatively impacts mass transport gradient especially at higher current densities [99]. Though considerable enhancement was achieved by using K_2CO_3 salt as discussed above to enhance the porosity and diffusion of O_2, a clear understanding of the catalyst shape and pore structure to engineer the catalyst layer of self-supported metal aerogel catalysts. In this regards Ishikawa et al [100] investigated the tomographic analysis of self-supported catalysts vs Pt black based catalysts to understand the porosity and its effects on O_2 diffusion. In comparison to Pt black, the Pt_3Ni aerogel CL shows considerably poorer O_2 mass

transport in PEFC experiments due to its small and twisted pores (<100 nm wide), which are larger and straighter (>100 nm wide). When applying Pt_3Ni aerogel in MEAs, it is clearly seen that the PEM performance is found to be lower than the Pt-black. indicated significantly poorer O_2 mass transport. The mass transport is enhanced by the addition of a pore precursor filler material, K_2CO_3 to the Pt_3Ni catalyst ink which enhances the porosity and increased power density [Figure. 3d]. Therefore, it is important to enhance the internal porosity with more straight pores that requires unique ideas to engineering the catalyst layer during the electrode preparation. Another important aspect of PEM fuel cells is the carbon support corrosion during under fuel starvation. During a start-up/shutdown of the fuel cell, potential can shoot up to more than 1.5 V vs RHE in cathode [101]. On the events of water blockage on the anode flow field or the complete loss of anode fuel under load conditions or anode catalyst layer flooding by water accumulation, leads to potential shoot up in the anode that leads to severe carbon corrosion at the anode side [102]. In this regard, self-supported catalysts could hold potential applications as anode catalyst due to their metallic nature with no carbon as the support. In a work by Henning et al [103] investigated the possibility of using Pt_3Ni metal aerogel electrocatalyst as corrosion resistant anode catalyst with a catalyst loading as low as 0.05 mg_{Pt}/cm^2. The Pt_3Ni, Pt/CB and Pt/GCB catalysts as anodes, are subjected to a fuel starvation condition that allows the anode potential to rise as high as 1.5 V vs RHE. Under this fuel starvation mimicking conditions, Pt/CB, Pt/GCB both suffered significant performance losses whereas Pt_3Ni metal aerogel catalyst showed almost no loss in the fuel cell performance. At the end of fuel starvation testing, the anode hydrogen oxidation overpotentials as found to be significantly higher for Pt/CB and Pt/GCB whereas for Pt_3Ni, the overpotential remains largely unchanged. This overpotential difference is due to the fuel starvation induced carbon corrosion phenomenon in CB and GCB based catalysts [Figure. 3 e,f]. This study clearly indicates that carbon corrosion is one of the major causes of PEM fuel cell degradation both in anode and cathodes. In this regard, self-supported metal aerogel catalysts find interesting applications both as anode and cathode catalysts owing to their completely metallic nature.

In a continuation work of Prof. Alexander Eychmüller research group [73,75,77,80] on extensive investigation of Pt_3Ni aerogel from the synthesis, compositional, topographical analysis, finally they applied the Pt_3Ni aerogel catalyst in a PEMFC in a realistic automative-relevant operating conditions to realize their importance in a realistic fuel cell condition. The DoE target of fuel cell should have a cost and performance target of $\leqslant$US$ 30/$kW_{net,stack}$ and $\geqslant$8000 h of on-road operation [104]. In this work, Firky et al [105], comprehensively investigated the long-term durability of the Pt_3Ni metal aerogel catalysts under realistic MEA conditions of fuel cells and cross verified the stability by various electrochemical characterization techniques. The contrasting differences in the traditional Pt/C cathodes vs Pt_3-Ni metal aerogel cathodes as shown in the Figure. 3g, h. The fuel cell polarization curves of Pt_3-Ni metal aerogel cathodes showed considerably good performance at relative humidity levels (RH) of 100% just like Pt/C, however, with lower RH, the performance slightly drops in relation to Pt/. Detailed CV studies indicate that the lower performance of Pt-Ni at low RH is due to the larger Pt-oxide coverage on Pt-Ni catalyst when compared to Pt/C catalyst. While studying the effect of temperature, it was found that increased temperature enhances the performance of both the catalyst layers owing to the enhanced reaction kinetics due to decreased activation energy, increased membrane condition of protons.

Inspired by the excellent activity, stability both in RDE and fuel cell conditions, further efforts were made to scale up the synthesis of the Pt_3Ni catalysts was achieved by Fikry et al [106]. By following the standard precursors ratio, the final aerogel catalyst obtained was around 23 mg. The standard reactant ratio was further up scaled by 5 times, with a slightly modified reaction scheme, employing slightly higher temperature to fasten the gelation that reduces the gelation time from 5-6 days to just 1 day and increasing the reaction volume, enhancing the solvent exchange with *tert*-butanol and replacing the CO_2 based super-critical drying with freeze drying. With these modifications, the entire synthesis process was shortened by 6 days with the aerogel yield of 125 mg, around 5.5 times higher yield. It is shown that use of *tert*-butanol leads to highly porous aerogels [107]. TEM image showed almost no visible differences in the morphology of Pt_3Ni catalyst in the standard and in the up-scaled synthesis process. Not only morphology, but the CV and RDE results also showed that the upscaled catalyst ECSA and specific surface area of the standard and up-scaled catalysts showed nearly identical activity suggesting that the catalyst activity can be retained with the modified synthesis scheme and show the potential to further improve to the gram levels. It is worth mentioning that both the standard method and the up-scaled synthesis method were able to achieve similar PEMFC performance. This suggests that there is a chance to scale up the synthesis process to meet commercial demands, as the results were comparable. [Figure. 3i-k].

While the traditional core-shell structured electrocatalysts made of Pt and transition metals are popular for their ability to maximize the Pt utilization and tuning the electronic structure of Pt by altering the d-band center therefore optimize the oxygen adsorption and reaction intermediates [108]. In addition, synthesizing the core-shell nanostructures necessitates the use of surfactants or stabilizers to fine tune the morphology and Pt shell thickness. However, using the surfactants or stabilizers in the metal aerogel catalysts synthesis obstruct the gelation step, thus leading to a denser structure with relatively low surface area. Therefore, the synthesis of core-shell structured metal aerogel catalysts are hardly reported. In this regard, Cai et al [87] developed a Pd_xAu-Pt core-shell structure which is composed of ultrathin Pt shells on the Pd_xAu core via a two-step synthesis method. After the Pd_xAu aerogels were made using a spontaneous gelation method, they were galvanically replaced with Pt and then conformally covered with a Cu monolayer via underpotential deposition method that resulted in $Pd_{10}Au$-Pt nanowires (Figure. 4a-e). It was found that ultra-thin Pt shells enhance the catalyst utilization and tune the electronic structures resulting in mass and specific activities as high as 18.7 and 4.1 times higher than those of Pt/C catalysts have been observed. In this work authors adopted a two-step method for the synthesis of core-shell metal aerogels that are composed of ultrathin layer of Pt shell on Pd_xAu core. A significant challenge in synthesizing core-shell type metal aerogels is the requirement for stabilizers. The utilization of stabilizers is crucial for regulating the dimensions of metallic nano building blocks; however, robust stabilizers impede the gelation process, while weak stabilizers inadequately manage it, resulting in a denser structure with comparatively low surface area. In this study, authors tactically solved this problem, with a conventional galvanic displacement reaction. First, the Pd_xAu were obtained by a spontaneous reduction-gelation mechanism, are covered by Cu atoms via underpotential deposition (UPD), which are then replaced with Pt atoms via a traditional galvanic displacement reaction, to obtain the ultra-thin Pt atoms. With a successful synthesis of this method, a similar process was then extended to other shell atoms such as Ni, Co and Cu. The obtained Pd_xAu-Pt core-shell structured metal aerogels exhibited a typical 3d- wire-based

backbone topology with thin Pt shell which boosts the Pt utilization [109]. The cyclic voltammetry (CV) results showed extraordinary electrochemical surface area of 192 $m^2\ g^{-1}_{Pt}$. The enhancement of Pt utilization efficiency was demonstrated by normalizing the kinetic current at 0.9 VRHE to the loading of both Pt and noble metals. The Pd_{20}Au-Pt core-shell aerogel exhibits a mass activity of 5.25 A mg^{-1} Pt, which is 18.7 times greater than Pt/C (0.28 A mg^{-1}Pt) [Figure. 4f-i]

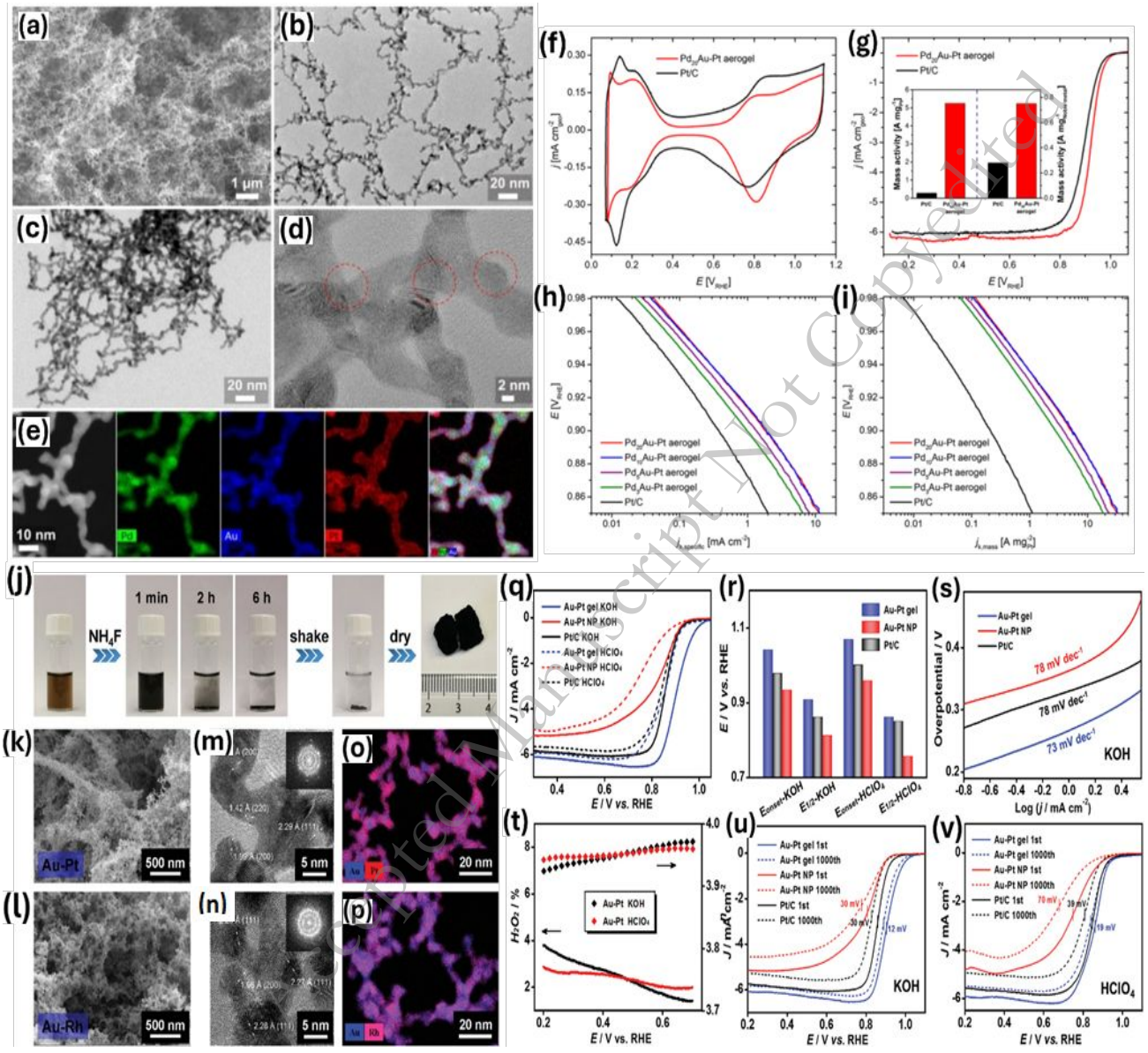

Figure 4. *(a) SEM (b-d) TEM (e) HAADF-STEM image and their corresponding EDAX element maps for Pd_{10}Au-Pt core-shell aerogel. (f) CV (g) LSV (inset: mass activity) curves, (h,i) tafel slopes of Pt/C and Pd_xAu-Pt core-shell aerogel catalysts respectively. [Reproduced with permissions from Ref. 87]. (j) schematic of aerogel catalyst synthesis, (k, l) SEM, (m, n) TEM, EDAX mapping of Au-Pt aerogel catalyst (o, p) SEM, TEM, EDAX mapping of Au-Rh aerogel catalyst (q) ORR curves (r) onset, half-wave potentials (s) tafel slopes (t) H_2O_2/number of electrons (u) stability curves in KOH (v) stability curves in $HClO_4$ of Au-Pt and Pt/C catalyst [Reproduced from Ref. 110, Open access].*

One of the important limitations of the metal aerogel catalysts is their tedious synthesis process including the inadequate destabilization of the metallic atoms to undergo gelation. In order to tackle this process, Du et al [110] introduced a salt-out method with a NH_4F as a gelation initiator, because of its strong salting-out capacity as dictated by the Hofmeister series to synthesize metal aerogel alloy catalysts [111]. The complex concentration processes described elsewhere can be skipped when using a dilute citrate-stabilized metal NP solution with a low metal concentration (cM = 0.2 × 10−3 m) as the precursor, all because of NH_4F high destabilization ability. Due to its strong salting-out capacity and destabilizing ability NH_4F, a quick reduction of Au-Pt nanoparticles and hydrogel formation was achieved within 6 hours. The Au-Pt metal aerogel was shown to have highly porous, branched and interconnected nanowire morphology with spatially distributed au and Pt atoms. Furthermore, NH_4F the synthesis process was further translated to other metal aerogel systems like Au-Pd, Au-Pt, Au-Rh and Au-Pd-Pt. Various metal aerogel catalysts are evaluated for HER, OER and ORR applications in a three-electrode system. The optimized Au-Pt metal aerogel catalysts were assessed for ORR in both acidic and alkaline electrolytes. The Au-Pt gel catalysts exhibited enhanced ORR activity surpassing the Pt/C catalyst with an onset and half-wave potential of 1.04 and 0.91 V vs RHE, respectively, especially in alkaline electrolyte and 1.07 V and 0.86 V in acidic electrolytes. In addition, the Au-Pt gel catalyst showed the lowest tafle slope (73 mV dec^{-1}) and nearly 4 electron O_2 reduction pathway [Figure. 4j-v]. In another study, Chen et al [112] proposed a $NaBH_4$ based reduction and stabilization method to synthesize Pt-Cu metal aerogel catalysts. Alloying Pt with Cu is beneficial because the strain and electron effects of Cu doping help to modify Pt [113]. The metallic aerogel was obtained after 5 h of the reduction of metal precursors with $NaBH_4$. TEM measurements revealed that PtCu aerogel is composed of 2 nm in diameter of spherical shape with a crystalline nature. The hierarchically porous structure of the as-prepared PtCu aerogels is accompanied by a high specific area of 33 m^2/g. The ORR activity is particularly noteworthy, with a mass activity of 369.4 mA/mgPt and a specific activity of 0.847 mA/cm^2, which are 2.6 and 3.3 times higher than the respective values for commercial Pt/C.

Tailoring the metal aerogel catalysts by controlling the metal distribution, composition and crystallinity remains the challenging task. This is due to the enormous, interconnected porous structure in the metal aerogels. In addition, the scale up of the metal aerogel catalysts is still a challenging issue. To address compositional control and scale up issues, Zheng [114] proposed a unique controlled synthesis strategy by using ambient O_2 etching strategy for the synthesis of $Pt_{83}Ni_{17}$ that results in the morphology of bunched-nanocages [Figure. 5]. In a typical synthesis, an aqueous solution of Pt and Ni processes are first reduced to metallic state by $NaBH_4$, which turns the solution into dark, due to the reduction of the metal precursors. After 10 minutes Pt-Ni hydrogel was formed as characterized by the fluffy solid, which was further allowed for 12h gelatinize to settle at 60°C. The resulting Pt-Ni hydrogel was further acid washed and dried in a supercritical CO_2 environment. The SEM images showed bunched nanocages (BNCs) with an average diameter of (11.8 ± 1.9) nm of the $Pt_{83}Ni_{17}$ BNCs AG catalyst. Interestingly, the TEM images show clearly the highly crystalline nature of the bunched nanocages with abundant grain boundaries in PtNi aerogel, that could benefit the O_2 reduction kinetics [115]. It is interesting to know that, just by simple Reduction of metal ions does not lead to core-shell nanoparticles, instead it should give an alloy of Pt and Ni. However, the transmission electron microscope of the $Pt_{83}Ni_{17}$ BNCs AG Catalyst presented a core-shell

nanostructure. The authors tried to understand the transformation of hydrogel into core shell nanostructures by performing a series of time dependent experiments and isolating the intermediate products at different stages. Precursor Pt-Ni hydrogel shows a morphology of solid nanospheres that are interconnected randomly with platinum has a shell and a nickel as a core, indicating that during the reduction process nickel ions reduced first to form the core and later the platinum ions are reduced to form the shells. However, based on the thermodynamic Standard reduction potentials the platinum reduction potentials are positive whereas the nickel reduction potentials are negative indicating that principally platinum should be reduced first followed by the nickel [116]. Authors try to understand the mechanism behind the difference in the reductions of metallic species based on nickel to platinum precursors feeding ratio. It was found that when the nickel 2 platinum feeding ratio is 3:1 results in the formation of platinum nickel alloy however when the feeding ratio increased to 4:1 and 6:1 they obtained Pt-Ni hydrogel precursor turned into a core-shell structures with nickel as a core and platinum as a shell. Interestingly when Pt-Ni hydrogel precursor is subjected to Increase in temperature at 60°C for two hours the solid core shell structures transformed into hollow nano cage structures. The hollow nano cage structures emerge more and more as the time increases at 60°C. The evolution of hollow nano cages from the solid nanospheres of Pt-Ni hydrogel is explained based on the ability of core nickel to interact with atmospheric oxygen on edge from the core and moves towards the platinum rich surface via Kirkendall effect [117]. Due to relative inertness of platinum to react with oxygen, nickel instead reacts with dissolved oxygen and therefore moves to the surface and reacts with hydroxide ions to form nickel hydroxide structures which are then later removed by the acid etching leads to the formation of bunched nanocage structures (Figure. 5g). The resulting $Pt_{83}Ni_{17}$ BNCs AG catalyst showed excellent ORR activity with a half-wave potential of 0.94 V vs RHE and mass activity (1.95 A $mgPt^{-1}$) specific activities (3.55 mA cm^{-2}) higher than 4.4 times the 2025 target of DoE (0.44 A $mgPt^{-1}$ at 0.90 V Vs RHE). In addition to the excellent ORR activity, the $Pt_{83}Ni_{17}$ BNCs AG catalyst also showed higher electron transfer number of 4.0 suggesting a direct, selective reduction of oxygen to H_2O and extraordinary stability with a negligible loss in half-wave potential after 20,000 accelerated durability tests in the potential range of 0.6 – 1.1 V vs RHE. Such a high durability of the $Pt_{83}Ni_{17}$ BNCs AG catalyst is also cross verified by the post TEM analysis, which show almost no visible deterioration of the core-shell structures even after 20,000 potential cycles, suggesting that $Pt_{83}Ni_{17}$ BNCs AG catalyst can be considered as one of the best alternatives to Pt/C catalyst [Figure. 5h,i]. In addition, the authors were able to scale up the synthesis process to gram level, therefore, the entire synthesis process can be scalable to meet the industrial scale for commercialization purposes.

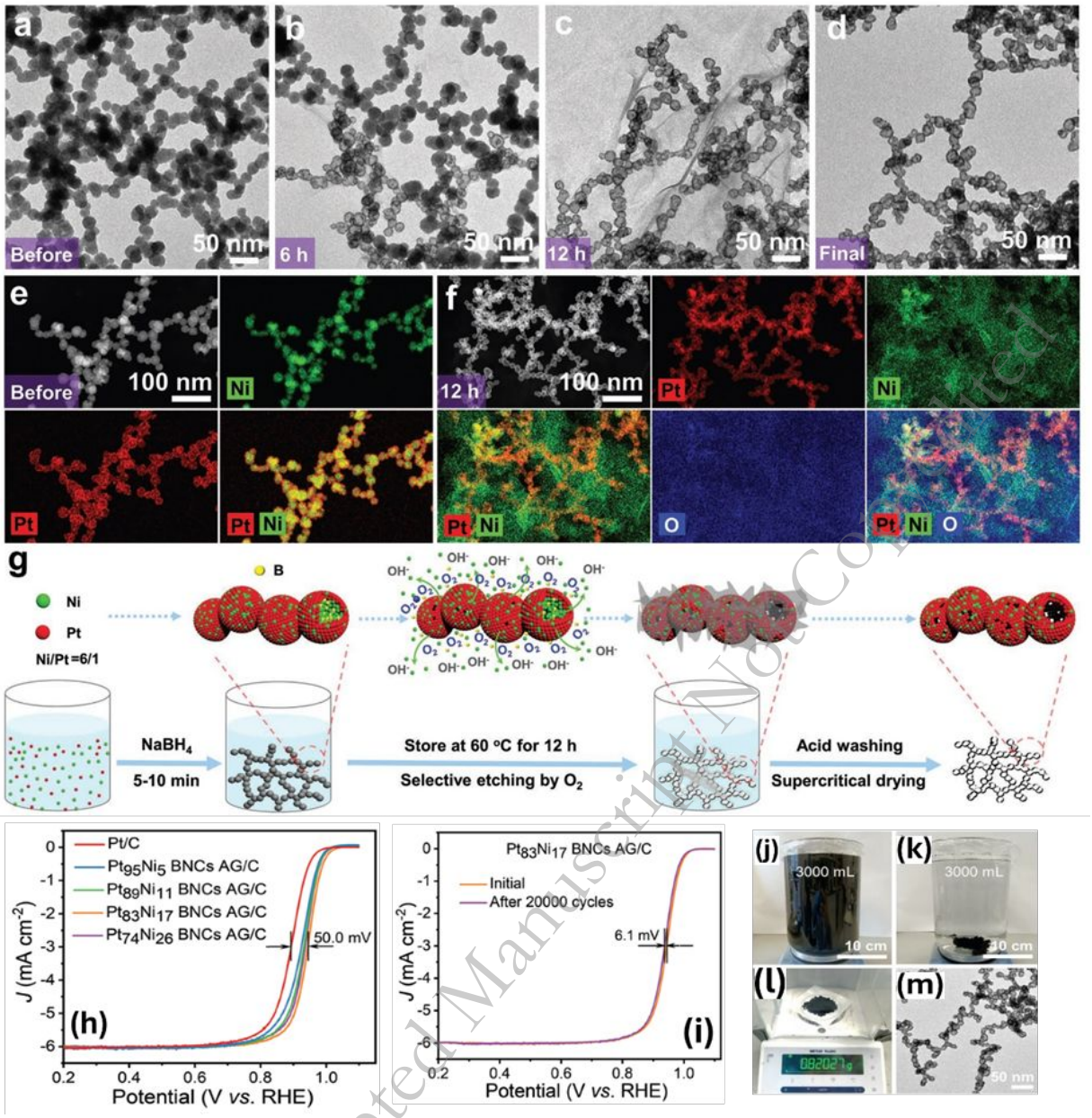

Figure 5. *(a-c) TEM images Pt-Ni hydrogel precursor recorded at different time intervals (d) the final $Pt_{83}Ni_{17}$ catalyst BNCs AG (e) HAADF-STEM images of the Pt-Ni hydrogel precursors before (f) after 12 h. (g) Schematic illustration of the formation mechanism of the $Pt_{83}Ni_{17}$ BNCs AG (h) ORR LSV curves of Pt/C and various compositions of Pt_xNi_y BNCs AG (i) ORR stability curves of $Pt_{83}Ni_{17}$ BNCs AG (j-l) gram level synthesis of $Pt_{83}Ni_{17}$ BNCs AG (m) TEM image of $Pt_{83}Ni_{17}$ BNCs AG synthesized in gram levels [Reproduced with permissions from Ref. 114]*

Cutting-Edge Metal Aerogel Design and Engineering

Morphology Engineering: It is well known that morphology of nanomaterials affects catalytic performance. No matter if the aerogels are made of a single metal or a combination, they all have a 3D network shape and results in nanowire morphology with $NaBH_4$ reduction method

via sol-gel route. However, some reports suggest the nanosheet, nanotubular, nanotube and nano shell morphology could also be achieved by modifying the aerogel synthesis procedures. It is generally assumed that influence of reducing agent and the synthesis method adopted could be directly linked to the morphology of the aerogel [70]. For example, IrCu core-shell structures are produced from the self-assembly of IrCu nanoparticles via GRR [118]. IrCu core-shell nanowires are produced by one-pot, surfactant free approach. It is observed that when the Cu and Ir precursors were reduced it forms the IrCu nanocrystals with Cu as the core metal. The Cu nanocore formation is possible due to the lower decomposition temperature and faster decomposition rate of the Cu^{2+} ions, despite the lower redox potential of Cu than the Ir. After about 5 min, nanovoids were observed on IrCu NCs, owing to the galvanic displacement reaction in which the Cu atoms from the core move outward and replace the Ir atoms, generating smaller NCs that later fused to form short chains which were further proceeded to ordered connection and fusion to form nanowires of core-shell structures with nanovoids (Figure. 6a) In another study, porous PtAg nanotubes have been obtained via GRR [86]. PdAu-Pt core-shell structures have been obtained by using UPD on PdAu hydrogel by Cu monolayer [87]. PdPb@Pd aerogel core-shell structures are obtained by using NaH_2PO_2 as a reducing agent [119], whereas CO as a reductant, results in Pd nanosheet aerogels [66]. Therefore, the synthesis of aerogels may be described as flexible since it can provide a wide range of morphologies depending on the reductants utilized and the modifications made to the synthesis process.

Facet Engineering: It is well known that nanomaterial properties are dependent on the size and orientation of the nanoparticles on facet [120]. Aerogel synthesis process helps to provide the opportunity to tune the nanoparticles of a particular facet. For example, Au nanoparticles of Au (100), Au (110), Au (111) facets have been synthesized with a desired nanoparticles size by Duan et al [121]. In this work, authors tried a unique fundamental phenomenon of nanoparticles fusing to generate the Au aerogels with a facet of {110} from Au {111} {100}{110} by mixing the two sizes of Au nanoparticles with different nanoparticles sizes of 16, 30 and 50 nm to the Au nanoparticles of 6 nm in size. It is generally believed that a low indexed crystalline facets if {111} and {110} are found predominantly on a spherical and quasi-spherical nanoparticle, whose ratio increases with increasing in particle size. Therefore, it can be assumed that when mixing nanoparticles of two different sizes, they would have different ratio of {111} and {110} and the nanoparticles tend to fuse together based on the surface free energies of each facet. When the nanoparticles are fused, they tend to form a new facet with the lowest surface energy. Based on this assumption, authors mixed Au nanoparticles of 6 nm with the Au nanoparticles solution of 16, 30 and 50 nm. While doing so, in $Au^{6\text{-}16}$ aerogels, 100} facets predominantly exist, whereas most {111} facets disappear, whereas in $Au^{6\text{-}30}$ and $Au^{6\text{-}50}$ aerogels, the original Au {100} facets disappear, and a high ratio of newly formed Au {110} facet appears instead. While looking at the surface free energies of Au {111}, Au {100}, and Au {110} facet, which are 1.52, 1.80, and 1.94 J m^{-2}, respectively, the transformation of {100} to {110} facet is highly possible, while fusing the Au nanoparticles of different sizes by size-dependent localized Ostwald ripening. The transformation of the facets are clearly established with the help of cyclic voltammogram (Figure. 6b,c). These results indicate that the aerogel synthesis process also allows tuning the nanoparticle size and selective facet over other facets, giving an immense potential of aerogel synthesis for electrocatalysis.

Composition Engineering: Elemental composition is a key strategy to control the properties of the metal aerogels which in turn influences electrocatalytic activity and the electronic behavior of the metallic system, which helps to tune the properties. Metal aerogels were initially proposed for monometallic aerogels, however, recently the synthesis process of multi-metallic aerogels have been well reported. For instance, the Pt-Pd aerogels exhibited the usual behavior of Pt clusters embedded in the Pd network backbone, while the Au−Pd aerogels showed that the Pd shell encased the Au-rich cluster. In contrast, the Au-Ag bimetallic aerogel exhibited typical alloy behavior [122]. This contrast is associated with the lattice parameter of different metals. Therefore, the synthesis of aerogels allows not only to synthesize single meal aerogels, but also to allow the compositional tuning of metal aerogels by allowing the formation of alloys with different metals, to tune the electrochemical properties. In addition to facilitating the synthesis of compositional alloys, aerogel synthesis aids in the embedding of atomically dispersed metals onto alloy-based nanomaterials. For example, galvanic replacement reaction (GRR), atomically dispersed Pd and Pt atoms are deposited on the AuCu hydrogels [123,124]. Therefore, a coupled strategy of atomically dispersed atoms on the hydrogel can be obtained, to compositionally tune the aerogels for electrocatalytic applications.

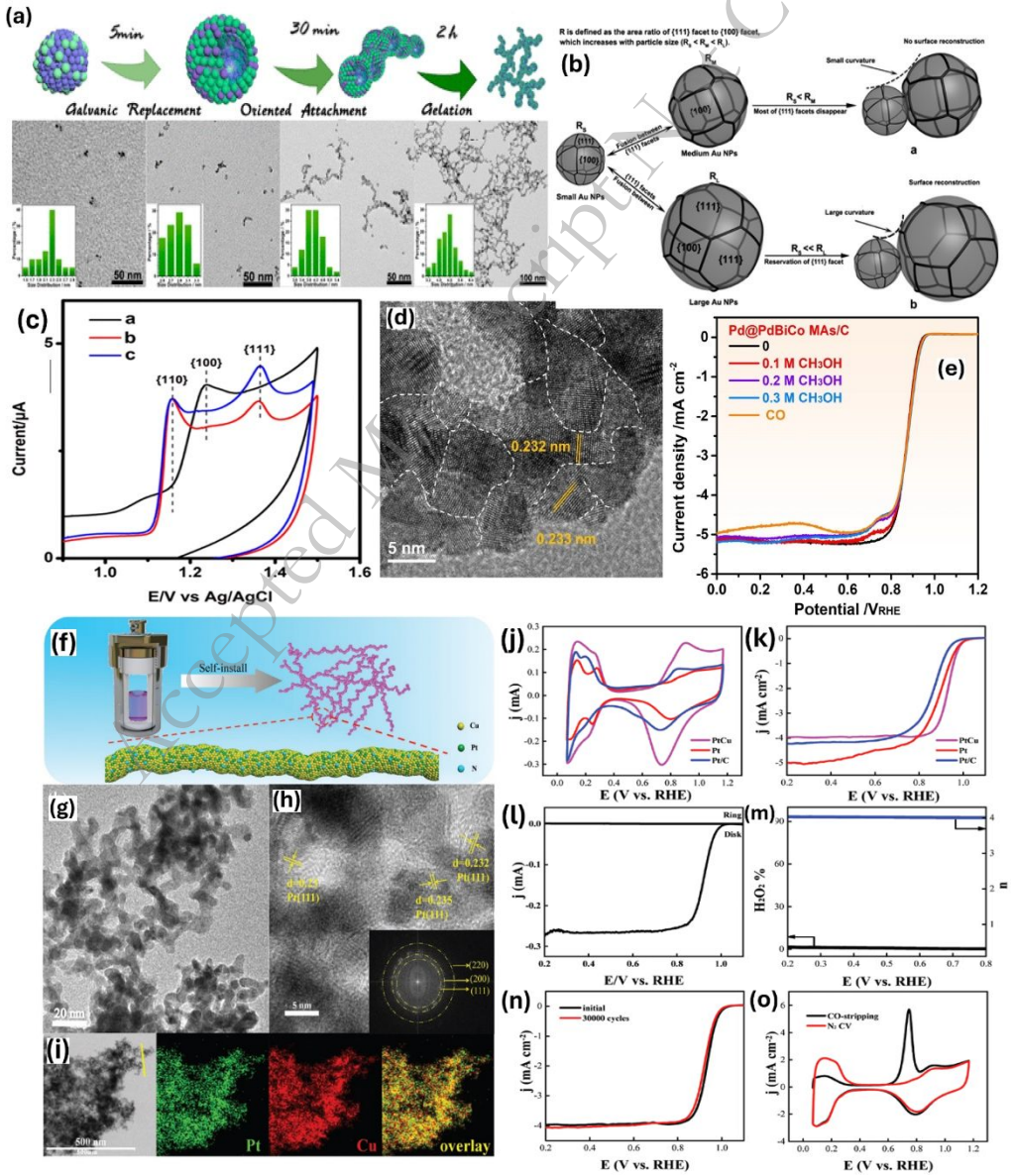

Figure. 6. *(a) Schematic representation of morphology evolution of nanovoid at different time intervals and their corresponding TEM images [Reproduced with permissions from Ref. 118] (b) pictorial representation of evolution of facets of Au NPs of two different sizes during the formation of Au^{m-n} aerogels without (a) and (b) with surface reconstruction (c) CV curves of Au^{m-n} aerogels on GCEs in 0.5 M H_2SO_4 at a scan rate of 50 mV s^{-1}: Au^{6-16} aerogels (a), Au^{6-30} aerogels (b), and Au^{6-50} aerogels [Reproduced with permissions from Ref. 121]. (d) HRTEM imagesof Pd@PdBiCo MAs (e) LSV curves of Pd@PdBiCo MAs/C [Reproduced with permissions from Ref. 125] (f) schematic catalyst synthesis (g-i) TEM, elemental mapping of PtCu catalysts (j) CV (k) LSV curves (l) ring currents (m) % of H_2O_2 (n) LSV stability LSV curves (o) CO oxidation analysis by CV of PtCu catalyst [Reproduced with permissions from Ref. 132].*

Lattice strain engineering: In a recent work, Fu et al [125] developed a lattice-strain induced Pd@PdBiCo quasi cores-hell metallic aerogel catalyst by a unique "one-pot and two-step" method for methanol and Co resistant ORR catalyst. Given its high-density of un-saturated surface atoms, surface suspended bonds, lattice distortions, and defects, engineering the metal alloys by manipulating the lattice strain is considered as highly effective method for achieving superior electro-chemical properties [126]. If the core metal and shell metal have different lattice parameters, then the core-shell structure is prone to the lattice strain effect; the extent to which the shells experience strain is proportional to the degree to which their lattice parameters are mismatched in the alloy [127]. The strain developed in the alloy modifies and enhances the interaction between oxygen and metallic active sites towards improved ORR activity [128]. In brief, the synthesis involves the preparation of metallic Pd nanoparticles in an ionic liquid assisted strategy, into the same reaction mixture, addition of Pd, Bi, Co salts and hydrazine as reducing agent has been added to obtain the final Pd@PdBiCo quasi cores-hell metallic aerogel within 30 minutes. The resulting trimetallic aerogel catalyst with individual atomic ration of 81.7/7.0/11.3 for Pd, Bi and Co, showed excellent surface area of about 144 m^2 g^{-1}. The Pd@PdBiCo metal aerogel catalyst showed a slight larger lattice spacings, caused by the tensile strain induced by the Bi and Co atoms in the crystal lattice [Figure. 6c,d]. However, this work contrast from the other metal aerogel works in such a way that, the synthesized The Pd@PdBiCo metal aerogels were loaded on the VulcanXC-72 R by dispersing via ultrasonication, whereas most of the other studies report to use self-supported metal aerogels as such as ORR catalysts. The ORR studies were conducted in 0.1 M KOH along with CO and CH_3OH as poisoning susbtacnes. In the ORR investigation studies, the commercial Pd/C and the control Pd MAs/C catalysts showed poor tolerance to ORR in the presence of poisoning substances, observed by the obvious methanol oxidation peaks, whereas Pd@PdBiCo metal aerogel catalyst presented excellent resistance to poisoning substances and selective towards ORR. Interestingly, the Pd@PdBiCo metal aerogels catalyst could resist the presence of methanol with a concentration as high as 0.3 M indicating its suitable use as cathode catalyst in direct methanol fuel cells. In addition, Pd@PdBiCo metal aerogels catalyst also showed higher half-wave potentials than the control samples indicating that tensile strain induced

microstructure of Pd@PdBiCo is beneficial not only to enhance the ORR activity but also to selectively reduce the oxygen in the presence of methanol and CO species [Figure. 6e]. In addition to the RDE results, the practical application of the Pd@PdBiCo metal aerogel catalysts was determined in the gas diffusion electrode cell that mimics the realistic membrane electrode assembly that consists of electrolyte, nafion membrane, gas diffusion layer and the catalyst layer with a gaseous O_2 flow. In a GDE cell, the Pd@PdBiCo metal aerogel catalysts exhibited higher ORR performance than the commercial Pd/C and Pd metal aerogel/C catalyst. Another study on strain engineering of PtCu alloy aerogel has been unveiled by Wang et al [129] which exhibited the mass and specific activities of 1.65 A/mgPt and 3.96 mA/cm^2.

Surface N-modification of aerogels: It is well known that modification of the catalyst surface with N functionalities enhances the electronic conductivity and improves stability of the catalyst via strong metal-carbon interactions i.e M-N-C (M=transition and noble metals) [130]. While the nitrogen doped carbons and M-N-C based transition metal-based catalysts are quite popular in the electrocatalysis of oxygen reduction [131], the N-doped metallic aerogel are not reported so far. Surface N-functionalization of then metallic aerogels is expected to modify the electronic nature of the metal active sites and therefore optimize the O_2 adsorption kinetics leading to enhanced ORR activity. However, principally the N dopants are normally introduced on the catalyst matrix by using the N containing ligands such as melamine, 2-methyl imidazole, urea etc. via high temperature decomposition. Principally, in the metal aerogel catalyst synthesis, it is not normal to use the N-containing organic ligands that might alter the gelation process. Moreover, metal aerogels are generally not subjected to high temperatures annealing, therefore, it is not possible to use organic ligands to introduce their surface N-functionalities. In this regard, Song et al [132] proposed a solvent-based N-surface functionalization of the PtCu aerogel via the decomposition of N-methyl pyrrolidone (NMP) in an alkaline environment. The N-surface functionalization of the PtCu aerogel was found to introduce M-N-C (M=Pt, Cu) type of bonds evident from the XPS analysis. In addition, the surface functionalization also found to enhance the ECSA, ORR activity and stability. Contrasting the traditional aqueous based reduction, authors used solvothermal method at 180 °C for 8 h, to synthesize PtCu aerogels in the presence of H_2O, NMP and NaOH. The NMP served as both a nitrogen source and a reducing agent to alter the surface nitrogen of the PtCu alloy catalyst. The successful N-functionalization of metal aerogel was ascertained from the XPS analysis where, the appearance of pyrrole-N and Cu-N functionalities indicates that organic solvent NMP is involved in the functionalization of the Pt-Cu catalyst [133,134]. The electrochemical characterization of the PtCu showed a high ECSA of 102 m^2 g^{-1} and 0.932 V vs RHE of the half-wave potential, MA and SA values for the PtCu catalyst (0.459 A $mgPt^{-1}$ and 0.45 mA cm^{-2}) and excellent durability. The positron density distribution simulation reveals that N introduction significantly modifies the electronic density around Pt and Cu therefore assisting in enhanced ORR activity [Figure. 6f-o]. Though the simulation results show the definite role of N, the authors did not compare the N-PtCu with the PtCu aerogel catalyst without N-functionalization. However, this work opens up a new avenue of the idea on surface functionalization of the metallic aerogels as a strategy to tune the electronic structure of the catalysts for improved catalytic activity.

Molecular Engineering of Noble Metal Aerogels:

Several metal aerogel catalysts have been developed in the past literature that focus on the modification in the synthesis process, compositional adjustments and morphological evolution. However, modifying the surface properties of metal aerogels have paid little to no attention. It is well known that surface characteristics of metal catalysts by ligands, would greatly affect their electrocatalytic behaviors [135,136]. For example, water splitting, carbon dioxide reduction, alcohol oxidation, and ORR are just a few of the electrocatalytic processes that have made extensive use of porphyrins, which are typically electrochemically active molecular catalysts. The effect of surface characteristics by using different type of ligands (ex. polyvinylpyrrolidone and beta-cyclodextrin) have been recently explored to enhance glucose and ethanol oxidations [137,138]. However, the effect of surface ligands on metal aerogels for ORR have not been investigated so far. In this regard, Yuan et al [139] developed a unique strategy to functionalize the Pt metal aerogel with FeTPyP ligand. The high conjugated, metalloporphyrin based FeTPyP ligand acts as destabilizing agent as well as functionalizing agent [Figure. 7a-c]. To the citrate stabilized Pt colloidal nanoparticles, the addition of FeTPyP, resulted in the destabilization of the Pt nanoparticles leading to the gelation, resulting in fluffy black solid appearing within 6h. Due to the adsorption of FeTPyP ligand, a strong electrostatic interaction established between the pyridine-N and metal nanoparticles that leads to effective gelation, suggesting that FeTPyP played a role of linker between NPs to form the interconnected nanochain networks during gelation [140,141]. The presence of FeTPyP ligands on the metal nanoparticles surface has been confirmed by FT-IR and the apparent signals of N and Fe elements from the energy-dispersive X-ray spectroscopy (EDS) and XPS analysis. The TEM results confirm no adverse effects of addition of FeTPyP on the morphology and size of Pt nanoparticles. In a comparative investigation, the order of ORR activity was found to be Pt/C < Pt NPs < pure Pt aerogel < Pt_{FeTPyP} aerogel. Further, Pt_{FeTPyP} aerogel catalyst showed a high ORR activity in wide range of pH range in acidic, alkaline and neutral environments, with the highest mass activity in alkaline pH followed by acidic and neutral pH. The enhancement in the ORR activity of Pt_{FeTPyP} aerogel catalyst was probed by density functional theory analysis, which primarily revealed that iron porphyrin plays a critical role in effectively adsorbing and activating oxygen during ORR [142]. The adsorption energy of the O_2 molecule on the surface of the PtFeTPyP aerogel is higher (1.71 eV vs 0.93 eV) than that of the Pt aerogel, indicating that the O_2 molecule is more easily adsorbed on the PtFeTPyP electrolyte [143]. The PDOS analysis revealed that there is an obvious electron transfer from Pt to FeTPyP via Pt-N bond leading to lowering of the d-band center for Pt_{FeTPyP} aerogel than the Pt, indicating that the Pt_{FeTPyP} aerogel possess improved ORR activity. Further activity improvement was done by employing $PtPd_{FeTPyP}$ aerogel catalyst that exhibited high MA of 1.47 A $mgPt^{-1}$ than the Pt/C and Pt_{FeTPyP} aerogel catalyst. This study marks the new avenue in the molecular engineering of the metal aerogel that could enhance the gelation of kinetics and enhance ORR activity. Similar work by the same author explored Iron (II) phthalocyanine (FePc) as a molecular ligand in Pt aerogel which showed similar enhanced results in ORR activity for Pt-FePc aerogel catalyst [144]. In another study [145] several organic ligands modulated the surface electronic structure of Pt-based noble metal aerogels (NMAs), including 4-methylphenylene, which increased ORR electrocatalysis. Theoretical calculations showed that 4-methylphenylene's interaction with surface metals lowers the energy barrier for O* to OH* and downshifts Pt's d-band center, increasing ORR intrinsic activity. Both Pt_3Ni and PtPd aerogels with 4-methylphenylene

decoration improved ORR activity and durability in various media. Interestingly, 4-methylphenylene modified PtPd aerogel had 0.952 V halfwave potential and 10.2 times mass activity of commercial Pt/C. This study explains how electronic structure affects ORR electrocatalytic properties, promoting functionalized NMAs as effective ORR catalysts.

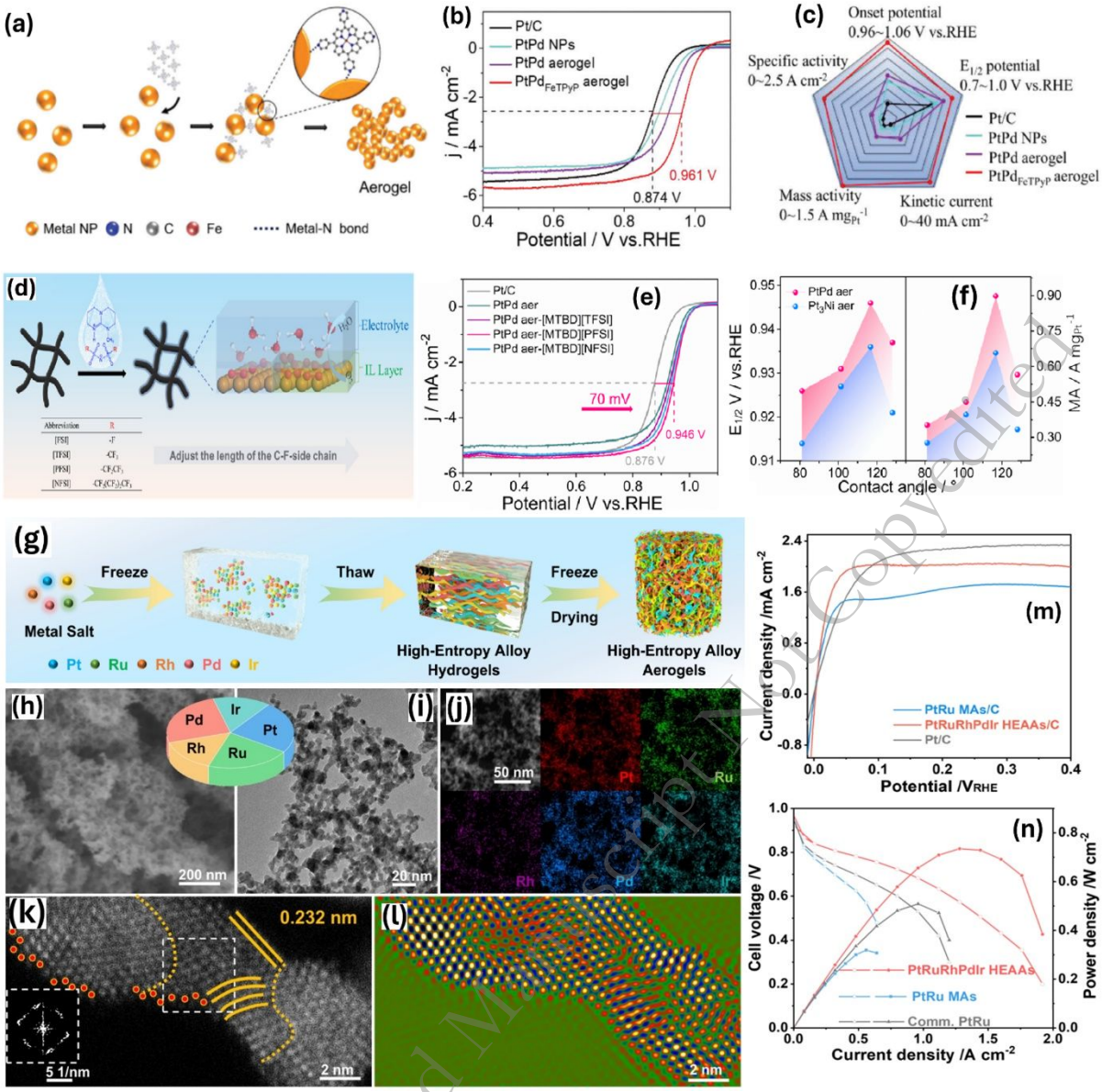

Figure. 7. *(a) Schematic illustration of the molecular engineering of NMAs (b) LSV curves of $PtPd_{FeTpyP}$ aerogel in 0.1 M KOH solution (c) onset, half-wave, mass activity, kinetic current and specific activity of various PtPd catalysts [Reproduced with permissions from Ref. 139] (d) Scheme for the synthesis of the Pt aer-ILs (e) ORR LSV curves of Pt/C, PdpD aerogel and PtPd aer-ILs in O_2-saturated 0.1 M KOH at 1600 rpm (f) Comparison of the $E_{1/2}$ and MA of the stated catalysts in 0.1 M KOH at 0.9 V versus RHE [Reproduced with permissions from Ref. 147] (g) schematic representation of high entropy alloy PtRuRhPdIr HEAAs catalysts (h) SEM (i) TEM (j) TEM-elemental mapping (k) AC-HAADF-STEM image (inset of FFT image), and (l) the corresponding inverse FFT image of PtRuRhPdIr HEAAs (m) HOR polarization curves (n) AEMFCs performance of PtRuRhPdIr HEAAs, PtRu MAs and the commercial PtRu [Reproduced with permissions from Ref. 159]*

Noble metal aerogels with surface hydrophobicity:

Surface design and modification can significantly impact electrocatalytic properties, which are closely linked to the physicochemical properties of electrocatalysts. Particularly, ORR is a solid-liquid-gas three phase reaction and the ORR activity of the electrocatalyst depends on the rate at this the O_2 diffuse from the bulk to the catalyst surface. The hydrophobic nature around the catalyst microstructure influences the O_2 dissolution and diffusion. Generally, considered that the optimum hydrophobicity is essential in the catalyst layer due to the fact that O_2 dissolves and diffuse through the hydrophobic region [146]. Based on this idea, Yuan et al [147] investigated ionic liquids (ILs) induced hydrophobic Pt-aerogel as ORR catalysts. To obtain the ionic liquid functionalized Pt-aerogel, first the Pt aerogels were prepared by gelation and freeze drying [Figure. 7d-f]. In a subsequent step, the Pt aerogel and ILs were re-dispersed and ultrasonicated in isopropanol solvent. After 12 h of settling time, which were then washed off and feezed tried again to obtain the Pt aer-[MTBD] [PFSI]. The Pt aer-ILs catalyst presents the morphology similar to the Pt aerogel catalyst. As expected, the C_{O2} in 0.1 M KOH is found to be higher than the C_{O2} in 0.1 M KOH. Results show that IL modification increases oxygen concentration on Pt aerogel surfaces, accelerating ORR progress [148]. Accordingly, the ILs functionalized Pt aerogel catalyst exhibited slightly higher ORR activity by 70 mV and Pt_3Ni aer-[MTBD] [PFSI] by 60 mV relative to Pt/C. In summary, the metal aerogel catalysts alone have found to have higher ORR activity than the Pt/C due to their porous structure and metallic nature. However, there are several opportunities to further engineer metal aerogels for enhanced activity by tuning the composition, surface engineering, oxygen adsorption kinetics, strain engineering and enhancing the electronic conductivity that could resolve the faster gelation and enhanced ORR activity and stability.

Highly Distorted High-Entropy Alloy Aerogels: It should be mentioned that electrocatalysts can exhibit distinct surface and lattice properties—like steps, defects, and suspended bonds through lattice distortion modulation. This allows for improved adsorption and activation of important electrocatalytic intermediates, as well as enhanced catalytic reactions due to an abundance of active sites and an increase in surface energy [149,150]. Particularly in high-entropy materials, where numerous elements typically occupy each sublattice, the electrocatalytic behavior is greatly enhanced by the unique atomic configurations that result from lattice disordering and increased configurational entropy [151-155]. Furthermore, metallic aerogels (MAs) are thought to have more active sites for electrocatalytic reactions due to their interconnected framework and distorted structures at the cross-linking points. This, in turn, should lead to efficient and stable operation, thanks to the abundance of step surfaces and lattice strain regions [156-158]. For the first time, Li et al [159] synthesized a high entropy alloy metal aerogels (HEAAs) that is composed of serval noble metals PtRuRhPdIr that possess unique structural characteristic of multiple lattice distortions, ultra-low density, high specific surface area, stability and conductivity. The HEAAs are prepared by a one-step synthesis process in which a mixture of metallic precursors is co-reduced by $NaBH_4$ reduction via freeze–thaw method [Figure. 7g]. The quick addition of $NaBH_4$ fastens the reduction of metal precursors in a confined spaces of ice crystals to generate a strong salting-out effect. The HEAAs atomic ratios obtained are consistent with the definition of the high-entropy alloy with 5-35 at %. In addition, the HEAAs synthesized in this work showed highest surface area of 189.88 $m^2\ g^{-1}$, one of the highest among several noble metal aerogels reviewed in this work.

The HEMAAs morphology shows a highly porous and fluffy nature. The lattice distortions and lattice mismatches can be clearly seen from the AC-HAADF-STEM and fast Fourier transform (FFT) images of the HEAAs. These lattice distortions and lattice mismatches in the HEAAs is due to the varying atomic sizes of the elements that also crats surface defects, which enhances the interaction with the reactants resulting in highest atomic utilizations. The clear evidence of lattice mismatches can be seen in the interfaces of three-dimensional cross-linked structures [Figure. 7h-l]. The synthesized HEAAs catalysts are evaluated for the hydrogen oxidation reaction (HOR) in H_2-saturated 0.1 M KOH at 1600 rpm. There is a remarkable increase in the HOR activity of PtRuRhPdIr HEAAs on carbon (PtRuRhPdIr HEAAs/C) compared to commercial Pt/C (0.34 A mg_{PGM}^{-1}) and 0.17 mA cm^{-2}, respectively, with a Pt group metal-normalized mass activity of 5.75 A mg_{PGM}^{-1}at 50 mV and an exchange current density normalized by electrochemical surface area of 0.69 mA cm^{-2} which is approximately 4.1 times higher than that of the Pt/C as anode catalyst in AEMFC. Impressively, the peak power density of a single cell with PtRuRhPdIr HEAAs MEAs reaches 0.73 W cm^{-2}, which is higher than those of the PtRu MAs and the commercial PtRu single cell [Figure. 7m,n]. These results indicate that HEAAs suitability as HOR catalyst. Nevertheless, the ORR activity of the HEAAs remains unexamined, presenting an opportunity for researchers to investigate further.

Conclusions

Metal aerogel self-supported catalysts have found to have excellent metallic nature and 3D porous network suitable for electrocatalytic applications. Due to their complete metallic nature, they possess excellent electronic conductivities and mechanical strength. Several metallic aerogels of Pt group metals and alloys of Pt group metals with transition metals have shown considerably higher ORR activity and excellent stability compared to Pt/C catalyst both in terms of mass and specific activities higher than the Pt/C and DOE 2025 recommendations and excellent stability over 20,000 potential cycles, with no loss in activity. These results indicates that aerogel catalysts possess excellent electrocatalytic activities. Metal aerogel catalysts are especially important in terms of their ability to mitigate the carbon corrosion when compared to traditional Pt/C catalyst, which is prone to undergo degradation under harsh, cathodic oxygen operating atmospheres. In addition to the role of cathode catalyst, the metal aerogel also found to have excellent resistance under the fuel starvation conditions, implying that metal aerogel catalysts can also function as anode catalysts. The 3D metallic network allows the complete utilization of the metallic framework for ORR; therefore, the metal aerogel often shows very high mass and specific activities compared to traditional Pt/C catalysts. Implying metal aerogel catalyst in the MEAs could significantly reduce the catalyst layer thickness to several orders of magnitude than the conventional Pt/C catalyst.

Key points

1. Metal aerogels possess excellent 3D networks that helps in enhanced mass transport of gaseous reactants and product water removal. This property helps in MEAs especially at higher currents.
2. Self-supported and self-conducting properties of metal aerogels makes the catalysts self-electronic conductive and hence do not require carbon supports. This property eliminates all the issues related to the catalysts stability concerning the carbon support, resulting in higher durability of the catalysts.

3. Metal aerogels exhibits higher utilization of metallic active sites due to the presence of uncoordinated metal atoms at the edges and steps of the metallic networks. This results in higher ORR activity due to their ability to adsorb the O_2 and optimized the O_2 adsorption energy and facilitate the direct 4 electron transfer.
4. Due to higher utilization of the metallic active site, the metal aerogel catalysts unusually exhibits 10-20 times higher mass activities compared to traditional Pt/C catalysts. This property significantly impacts positively on the catalyst cost.
5. The key limitation of the aerogel catalysts is the uneven distribution of ionomer in the 3D network reduces the abundance of three-phase boundaries. This requires careful optimization and novel strategies for ionomer distribution in the MEAs.

Limitations and challenges of metal aerogels

1. Synthesis-reproducibility is one of the major limitations of metal aerogel based electrocatalysts. The metal aerogel catalysts are primarily synthesized based on chemical reduction of metallic precursors to self-assembled metallic network, followed by the gelation process. The solution chemistry behind metal aerogel synthesis is sensitive to concentration of precursor solution/reductant, rate of reduction, solvent concentration and polarity and gelation time. Any variation could lead to structural variation of metallic product, structure-activity relationship This requires careful attention and hence the scalability at industrial levels is challenging.
2. During gelation step, the compositional changes might occur especially dealing with the noble metal-transition metal alloy aerogels, for example. This is due to the intrinsic variation of the metallic species and their ability to oxidize or dissolve. This might create a compositional gradient in the metallic networks, leading to the loss of induced electronic effects on electrocatalysis of ORR.
3. The 3D metallic networks of metal aerogels mechanically undergo disintegration/structural collapse during the catalyst ink-preparation or hot-pressing conditions. Therefore, the porous 3D network in the catalyst layer matters more than the structural morphology at the microscale levels.
4. Though, the metal-aerogel catalysts produce unusually high mass activities higher than 10-20 times of Pt/C, it is not entirely translated into reality in MEA levels. This is due to the gas-phase oxygen transport that is not reflected in the RDE studies. Futher, the pore filling of metal-aerogels with ionomer reduces the accessibility of recants and hence contribute to the high-mass transport resistance in the MEA level.
5. Another important limitation of the metal-aerogels in a realistic fuel cell is their lower density leading to the very thin catalyst layers, while increasing the catalyst layers crates additional resistance to the accessibility of gases reactants.
6. There are not many critical studies that dedicated the durability of metal-aerogels against dissolution/surface oxidations on start-up/shut-down conditions when potentials go over 1.4 V. Critical understanding and mechanistic studies are required to understand their structural stability and integrity against dissolution/migration/aggregation/Ostwald ripening/sintering/coarsening.

Future perspectives

1. One of the limitations of metal aerogel synthesis in large quantities (gram levels) is the substantially prolonged gelation required time. Despite attempts to decrease the prolonged gelation periods from several days to one day, and in certain instances to a few hours, it is crucial to devise innovative strategies to expedite the gelation process.

2. Currently, there are no studies examining the effects of various metal precursor salts, including nitrates, subphases, and acetates. It is crucial to understand the impact of counter ions on the destabilization of nanoparticles that leads to gelation. For instance, the introduction of common ion salts to the solution post-reduction may alter the ionic strength, potentially resulting in the precipitation or gelation of the nanoparticles due to the common ion effect. Experimental and modeling studies are necessary to elucidate the relationship between gelation and the counter ions of the precursors.

3. The current synthesis processes for metal aerogels are restricted to approximately ten elements, primarily from the platinum group metals, and for alloys, only a limited number of transition metals in conjunction with platinum group metals are investigated. It is imperative to broaden the synthesis process to include additional d-block elements, potentially in conjunction with lanthanides and platinum group metals. Although it is widely recognized that certain rare earth metals from the lanthanide series demonstrate exceptional ORR activities, no investigations have been conducted on rare earth metal aerogels for ORR studies. Consequently, it presents a valuable opportunity to study the metal aerogels of lanthanides and other d-block elements alone or in combination with the noble metal groups not only for ORR but also for other electrocatalytic reactions.

4. Modifying the composition of the aerogels is an effective strategy for adjusting the d-band center of the metal catalyst to optimize oxygen adsorption energy and density of states. This is achievable solely through an in-depth comprehension of the gelation mechanism for various metals, facilitating the regulation and manipulation of the rate-determining step to enhance gelation kinetics with controllable size, morphology, and potentially a desired facet.

5. One strategy to improve the ORR activity of metal aerogels is through surface modification with nitrogen atoms, which can strengthen the M-N bonding in the metal aerogels, thereby enhancing conductivity and the benefits of nitrogen doping. Thus far, only one study has been undertaken in this area utilizing the solvent as the nitrogen doping agent. We propose investigating alternative nitrogen modification strategies, such as treating metal aerogels in an ammonia atmosphere, and extending surface modification concepts to include other heteroatom dopants like sulfur, phosphorus, boron, and fluorine, as these approaches could substantially improve the oxygen reduction reaction activity and stability of metal aerogels.

6. Beyond surface modifications, metal-aerogels with core-shell structures is believed to further reduce the noble metal contents. And in addition, metal aerogels with core-shell structures in combination with transition metals, rare-earth metals further enhance and optimize the O_2 adsorption energy, stabilization of the metal aerogel against coalescence.

7. It is well known that metal-metal oxides/nitride heterojunctions enhances the ORR activity and stability of Pt-based ORR catalysts. It is reasonable to explore the possibility of metal-oxide/nitride in combination with the metal-aerogels which could result in highly stable ORR electrocatalysts.

8. Strain engineering of metal aerogels could be another alternative method to optimize the O_2 adsorption kinetics and therefore enhance ORR activity. Strain engineering can be done either by selecting TM or rare earth metal during the synthesis process or by employing unique post synthetic chemical/thermal methods. Defects engineering and surface re-construction of metal aerogels via plasma treatment or electrochemical potential cycling might also create defects that could serve as ORR active sites.

9. Surface modification of metal aerogels with electron donating or electron withdrawing ligands could be another way of enhancing the ORR activity of metal-aerogel catalysts. The legends not only modulate the electron distribution on the metallic active sites they also Stabilize the surface un-coordinated metal atoms.

10. Recently, high entropy alloys (Pt, Ru, Rh, Pd and Ir) based on metal aerogels were proposed for highly efficient hydrogen oxidation reactions in AEM fuel cells. It is interesting to explore the concept of high entropy alloys to the ORR possibly with a combination of noble metals with transition metals and/or lanthanides to tune the composition of high entropy metal aerogel alloys.

11. One of the primary challenges in integrating metal aerogels into membrane electrode assemblies is their impact on catalyst porosity. Regarding the transport of reactant and product water, it is essential for catalyst layers derived from self-supported catalysts to possess suitable porosities and pore size distributions to facilitate diffusion between active sites and the gas diffusion layer, like conventional catalyst layers prepared with carbon-supported catalysts. In case of carbon supported catalysts, large carbon agglomerates create void pores to facilities the diffusion of the reactant and product water. However, in the case of un-supported metal aerogel catalysts, there only exists a smaller agglomerate that might alter the mass transport and water management issues in the catalyst slayer that needs great attention. The knowledge of mass transport resistance is understanding in terms of pore dimensions, porosity and pore distribution in the catalyst of carbon supported catalysts and self-supported catalysts differ significantly. Therefore, a clear understanding of modelling studies coupled with experimental validations are highly required.

12. In order to incorporate the metal aerogel catalysts, it is essential to fabricate the MEAs based on CCM (catalyst coated membranes). In this regard, it is important to optimize the catalyst loadings, catalyst to nafion (ionomer) ratio and density of the catalyst ink, consistently which requires extensive research. So far there have been no studies dedicated in this direction.

Acknowledgements

The research was supported by the National Research Foundation of Korea (NRF) and funded by the Korean Government, Ministry of Science and ICT (MSIT) (No. 2021R1F1A1046648),

Republic of Korea. This work was partially supported by the National Research Foundation of Korea (NRF) grant funded by the Korea government (MSIT) (2021R1F1A1061143). Authors also thank the National Natural Science Foundation of China (Grant No. 12564010) and the General Project of Ganzhou Municipal Key Research and Development Program (Grant No. 2023PCG17009)

Conflicts of Interest

The authors declare no conflicts of interest.

Table 1 Physicochemical and Electrochemical kinetic data of various metal aerogel catalysts

Catalyst	Surface area ($m^2\ g^{-1}$) and Porosity	ORR activity				Durability	Ref
		ECSA $m^2\ g^{-1}_{Pt}$	Half-wave potential (V vs RHE)	Mass activity (mA mg Pt^{-1})	Specific Activity mA/cm^2	Potential cycling number of cycles / losses in $E_{½}$ (or) Chronoampero metry	
Pt_3Ni	80	31		≈62±5A/gPt @ 0.95 V ≈422 ± 34 A/gPt @0.90 V	200 µA ± 20	NR	[65]
$Pd_{20}Au$-Pt core-shell	83 to 105 meso- and macropores	192 $m^2\ g^{-1}_{Pt}$	0.922	5.25 A mg^{-1}_{Pt} @0.90 V 18.7 times higher than Pt/C	2.53	NR	[87]
Au-Pt gel	63.9–95.8 pore volumes (0.339–0.640 $cm^3\ g^{-1}$)	NR	0.91	0.37 A mg^{-1}_{Pt} @0.90 V 1.7 times higher than Pt/C (0.1 M KOH) 0.12 A mg^{-1}_{Pt} @0.90 V 15% lower than Pt/C (0.1 M $HClO_4$)	0.88 0.61	1000 / 12	[78]
$Pt_{83}Ni_{17}$ BNCs AG	58.4 pore volumes (0.09 $cm^3\ g^{-1}$) 5-7 nm pores	55	0.94	1.95 A mg^{-1}_{Pt} 8.9 times higher than Pt/C @0.9 V 4.4-times higher than 2025 DOE target	3.55	20,000 / 6.1	[114]
Pt-Ni upscaled	80	30	NR	≈56±7A/gPt @ 0.95 V	174 ± 13 µA cm^{-2}	NR	[106]
PtCu	NR	102.04	0.932	0.459 A mg_{Pt}^{-1} @ 0.90 V	0.45	10,000 / 24	[132]
Pd@PdBiCo MAs/C	144.83	NR	0.874	1.034 A mg_{Pd}^{-1} @ 0.85 V	NR	8000 / no loss	[125]

Pt_{FeTpyP} aerogel	106	66.2	0.942	□ 0.42 A mg^{-1}_{Pt} @0.9 V	□ 0.65	5000 / 9	[139]
Pt aer-FePc	NR	71.5	0.931	□ 0.25 A mg^{-1}_{Pt} @0.9 V	□ 0.39	5000 / 6	[144]
Pt aer-[MTBD][PFSI]	NR	65.9	0.946	0.581 A mg^{-1}_{Pt} @0.9 V	0.881	5000 / 7	[147]
PtPd aer-C=C	84	72.1	0.952	0.57 A mg^{-1}_{Pt} @0.9 V	0.79	5000 / 8	[145]
$Au_{52}Cu_{48}$	38.4	106 $m^2g^{-1}_{Au}$ 75 $m^2g^{-1}_{Pt}$	0.868	0.960 A mg^{-1}_{Au} at 0.85 V	0.906	3000 / 1 10,000 / 5	[160]
Pt-Cu aerogel	33	43.6	0.926	369 mA/mgPt	0.847	5000 / 20	[112]
Pd_3Cu aerogel	44.35, 8.77 nm, 0.094 $cm^3\ g^{-1}$ pore volumes	C_{dl} of 8.0 $mF.cm^{-2}$,	0.90	NR	NR	1700 / 13	[161]
$Pd_3CuF_{0.5}$	75.19, 15.29 nm pores 0.029 $cm^3\ g^{-1}$ pore volumes	C_{dl} of 21.9 mF cm^{-2}	0.92	NR	NR	16,000 s / 17.6% of relative current by CA	[162]
Pd_3Pb	142.8, 13 nm	NR	0.862	0.084 A mg^{-1}_{Pd}	NR	10,000 / 0.7 % of loss in half-wave potentials	[163]
Pd_4Au_3 MAs/C	NR	55	0.921	1.74 A mg^{-1}_{Pt} @0.9 V Exceeds DOE (0.44 A mg^{-1}_{Pt})	3.15	20,000 / 2	[164]
Palladene$_{50}$ aerogel	65.9	44.10	0.93	0.34 A mg^{-1}_{Pd} @0.85 V	□ 1.05	10,000 / 29	[165]
Au_2Cu	NR	8.9 $mF{\cdot}m^{-2}$	0.85	1.03 $A{\cdot}mg^{-1}_{Au}$ @ 0.85 V	j_k 5.3 $mA.cm^{-2}$	5000 / no loss	[166]
Pd_3Cu@2NC-20%	98	C_{dl}=12 mF cm^{-2}	0.925	NR	NR	15,000 s/ no loss	[167]
Pt_1Cu_2 AAs	NR	41.7	0.923	1.65 A/mgPt @ 0.90 V 7.9 times of Pt/C, higher than DOE 2025 target	3.96	10,000 / 2	[129]

References

1. H.A. Ibrahim, M.K. Ayomoh, R.C. Bansal, M.N. Gitau, V.S.S. Yadavalli, and R. Naidoo, Sustainability of power generation for developing economies: A systematic review of power sources mix, *Energy Strateg. Rev.*, 47(2023), p. 101085
2. H.C. Lau and S.C. Tsai, Global decarbonization: current status and what it will take to achieve net zero by 2050, *Energies*, 16(2023), p. 7800
3. Q. Zhou, Z. Liu, X. Wang, Y. Li, X. Qin, L. Guo, L. Zhou, and W. Xu, Co_3S_4-pyrolysis lotus fiber flexible textile as a hybrid electrocatalyst for overall water splitting, *J. Energy Chem.*, 89(2023), p. 336
4. J. Zou, L. Li, N. Tan, K. Zhang, L. Wang, and Z. Chen, Construction of S-scheme heterojunction with interfacial chemical bonds for enhanced photocatalytic CO_2 reduction, *Appl. Surf. Sci.*, 719(2025), p. 165001
5. Y. Cui, Y. Wang, B. Li, Y. Sui, G. Wang, J. Huo, J. Li, J. Huang, Y. Du, Z. Yu, J. Sun, and S. Jiang, Grain boundary segregation engineering in high-entropy multiphase alloys for overall water splitting at ultra-high current density, *Appl. Catal. B: Environ.*, 383(2025), p. 126035
6. T. Abedin, J. Pasupuleti, J.K.S. Paw, Y.C. Tak, M. Mahmud, M.P. Abdullah, and M. Nur-E-Alam, Proton exchange membrane fuel cells in electric vehicles: Innovations, challenges, and pathways to sustainability, *J. Power Sources*, 640(2025), p. 236769
7. Y. Nie, M. Uddin, Q. Wang, X. Li, N. Liu, S. Yu, P. Keomeesay, X. Zhao, Y. Chen, Z. Zheng, and S. Liu, Recent progress in Pt-based alloy catalysts: a comprehensive review on green synthesis and sustainable biomass hydrogenation applications, *Green Chem.*, 27(2025), p. 12070
8. Y. Zhou, W. Guo, L. Xing, J. Li, N. Wang, L. Meng, S. Ye, X. Yang, H. Chen, L. Du, and S. Ye, Stability and durability challenges of cathode catalysts for PEM fuel cells: experiments, mechanisms, and perspectives beyond three-electrode systems, *Energy Environ. Sci.*, 18(2025), p. 9054
9. Z. Liu, B. Peng, Y.-H.J. Tsai, A. Zhang, M. Xu, W. Zang, X. Yan, L. Xing, X. Pan, X. Duan, and Y. Huang, Pt catalyst protected by graphene nanopockets enables lifetimes of over 200,000 h for heavy-duty fuel cell applications, *Nat. Nanotechnol.*, 20(2025), p. 807
10. S. Zaman, L. Huang, A.I. Douka, H. Yang, B. You, and B.Y. Xia, Oxygen reduction electrocatalysts toward practical fuel cells: progress and perspectives, *Angew. Chem. Int. Ed.*, 60(2021), p. 17832
11. X. Deng, L. Ma, C. Wang, H. Ye, L. Cao, X. Zhan, J. Tian, and X. Tong, Recent progress in materials design and fabrication techniques for membrane electrode assembly in proton exchange membrane fuel cells, *Catalysts*, 15(2025), p. 74
12. R. Hong, L. Xing, F. Huang, Y. Chen, P. Li, X. Fang, M. Zhao, H. Ren, Z. Dong, Y. Yang, L. Du, and S. Ye, Scaling up membrane electrode assemblies for industrial applications, *Chem Catal.*, 5(2025), p. 101463
13. C. Lim, A.R. Fairhurst, B.J. Ransom, D. Haering, and V.R. Stamenkovic, Role of transition metals in Pt alloy catalysts for the oxygen reduction reaction, *ACS Catal.*, 13(2023), p. 14874
14. Z. Zhou, H.-J. Zhang, X. Feng, Z. Ma, Z.-F. Ma, and Y. Xue, Progress of Pt and iron-group transition metal alloy catalysts with high ORR activity for PEMFCs, *J. Electroanal. Chem.*, 959(2024), p. 118165
15. F. Kong, Y. Huang, X. Yu, M. Li, K. Song, Q. Guo, X. Cui, and J. Shi, Oxygen vacancy-mediated synthesis of inter-atomically ordered ultrafine Pt-alloy nanoparticles for enhanced fuel cell performance, *J. Am. Chem. Soc.*, 146(2024), p. 30078.

16. F. Zhan, K. Hu, J. Mai, L. Zhang, Z. Zhang, H. He, and X. Liu, Recent progress of Pt-based oxygen reduction reaction catalysts for proton exchange membrane fuel cells, *Rare Met.*, 43(2024), p. 2444
17. R. Ahluwalia, X. Wang, K. Chen, X. Wang, and J.S. Spendelow, Performance and durability of heavy-duty fuel cell systems with an advanced ordered intermetallic ORR alloy catalyst and novel support, *J. Electrochem. Soc.*, 171(2024), p. 114512
18. S. Shin, E. Lee, J. Nam, J. Kwon, Y. Choi, B.J. Kim, H.C. Ham, and H. Lee, Carbon-embedded Pt alloy cluster catalysts for proton exchange membrane fuel cells, *Adv. Energy Mater.*, 14(2024), p. 2400599.
19. F. Qian, C. Hu, W. Jiang, J. Zhang, L. Peng, L. Song, and Q. Chen, General and scalable strategy for synthesis of Pt–rare earth alloys as highly durable oxygen reduction electrocatalysts, *Chem. Eng. J.*, 468(2023), p. 143665
20. D. Liao, G. Tian, F. Xiaoyu, Z. Li, Y. Sun, W. Chang, Z. Li, L. Li, C. Zeng, F. Wei, and C. Zhang, Toward an active site–performance relationship for oxide-supported single and few atoms, *ACS Catal.*, 15(2025), p. 8219.
21. R. Zhang, J. Sun, Y. Chen, Q. Shen, C. Ding, S. Zhang, and J. Zhang, Advanced porous platinum group metal nano-structural electrocatalysts for water electrolysis, fuel cells and metal-air batteries, *Coord. Chem. Rev.*, 543(2025), p. 216958
22. S. Huang, Y. Shen, A. Li, H. Zhou, Y. Qiao, A. Yuan, H. Zhou, and S. Zheng, Dual-template synthesis of CoNi alloy nanoparticles anchored on N-doped carbon nanotubes for efficient oxygen reduction reaction, *Int. J. Miner. Metall. Mater.*, 32(2025), p. 3043.
23. Z. Xie, D. Zhang, H. Peng, Y. Lei, B. Yang, and F. Liang, Nitrogen-doped single-walled carbon nanohorns as Pt catalyst carrier: balance of strong durability and high activity of ORR, *Int. J. Miner. Metall. Mater.*, 32(2025), p. 2260.
24. M.A.A.M. Nor, M.A.A.A. Rani, K.S. Loh, T.F. Choo, K.L. Lim, S.H. Osman, A.C.M. Loy, and W.Y. Wong, Maximizing oxygen reduction reaction performance with minimal Pt: a review of high mass activity Pt–M catalysts, *J. Power Sources*, 654(2025), p. 237869
25. D. Banham and S. Ye, Current status and future development of catalyst materials and catalyst layers for proton exchange membrane fuel cells: an industrial perspective, *ACS Energy Lett.*, 2(2017), p. 629.
26. G. Wang, Z. Yang, Y. Du, and Y. Yang, Programmable exposure of Pt active facets for efficient oxygen reduction, *Angew. Chem.*, 131(2019), p. 15995.
27. Y. Chen, T. Cheng, and W.A. Goddard III, Atomistic explanation of the dramatically improved oxygen reduction reaction of jagged platinum nanowires, 50 times better than Pt, *J. Am. Chem. Soc.*, 142(2020), p. 8625.
28. Z. Wang, Y. Liu, S. Chen, Y. Zheng, X. Fu, Y. Zhang, and W. Wang, Strain engineering of Pt-based electrocatalysts for oxygen reduction reaction, *Front. Energy*, 18(2024), p. 241.
29. F. Ando, T. Tanabe, T. Gunji, S. Kaneko, T. Takeda, T. Ohsaka, and F. Matsumoto, Effect of the d-band center on the oxygen reduction reaction activity of electrochemically dealloyed ordered intermetallic platinum–lead nanoparticles supported on TiO_2-deposited cup-stacked carbon nanotubes, *ACS Appl. Nano Mater.*, 1(2018), p. 2844
30. L. Liu, J. Hu, X. Rao, et al., Revealing the dependence of oxygen reduction mechanism and activity on the d-band center difference of Fe–M bimetallic sites, *Appl. Catal. B: Environ.*, 384(2025), p. 126191.
31. M. Liu, Z. Zhao, X. Duan, and Y. Huang, Nanoscale structure design for high-performance Pt-based ORR catalysts, *Adv. Mater.*, 31(2018), p. 1802234.

32. W. Li, B. Weng, X. Sun, B. Cai, R. Hübner, Y. Luo, and R. Du, A decade of electrocatalysis with metal aerogels: a perspective, *Catalysts*, 13(2023), p. 167.
33. T. Vo, J. Gao, and Y. Liu, Recent development and future frontiers of oxygen reduction reaction in neutral media and seawater, *Adv. Funct. Mater.*, 34(2024), p. 202314282.
34. Z. Fang, C. Peng, Q. Zhou, and Z. Liu, Electrocatalytic hydrogen peroxide production: advances, challenges, and future perspectives, *Chem. Rec.*, 25(2025), p. e202500066.
35. R. Ma, G. Lin, Y. Zhou, Q. Liu, T. Zhang, G. Shan, M. Yang, and J. Wang, A review of oxygen reduction mechanisms for metal-free carbon-based electrocatalysts, *Npj Comput. Mater.*, 5(2019), p. 77
36. S. Li, L. Shi, Y. Guo, J. Wang, D. Liu, and S. Zhao, Selective oxygen reduction reaction: mechanism understanding, catalyst design and practical application, *Chem. Sci.*, 15(2024), pp. 11188
37. X. Ge, A. Sumboja, D. Wuu, T. An, B. Li, F.W.T. Goh, T.S.A. Hor, Y. Zong, and Z. Liu, Oxygen reduction in alkaline media: from mechanisms to recent advances of catalysts, *ACS Catal.*, 5(2015), pp. 4643
38. H.A. Gasteiger, S.S. Kocha, B. Sompalli, and F.T. Wagner, Activity benchmarks and requirements for Pt, Pt-alloy, and non-Pt oxygen reduction catalysts for PEMFCs, *Appl. Catal. B: Environ.*, 56(2004), pp. 9
39. B. Cai, S. Henning, J. Herranz, T.J. Schmidt, and A. Eychmüller, Nanostructuring noble metals as unsupported electrocatalysts for polymer electrolyte fuel cells, *Adv. Energy Mater.*, 7(2017), p. 1700548.
40. J. Zhao, Z. Tu, and S.H. Chan, Carbon corrosion mechanism and mitigation strategies in a proton exchange membrane fuel cell (PEMFC): a review, *J. Power Sources*, 488(2021), p. 229434.
41. S.G. Peera, R. Koutavarapu, S. Akula, A. Asokan, P. Moni, M. Selvaraj, J. Balamurugan, S.O. Kim, C. Liu, and A.K. Sahu, Carbon nanofibers as potential catalyst support for fuel cell cathodes: a review, *Energy Fuels*, 35(2021), p. 11761
42. B. Cai and A. Eychmüller, Promoting electrocatalysis upon aerogels, *Adv. Mater.*, 31(2018), p. 1804881.
43. L. Sun, Z. Jiang, B. Yuan, S. Zhi, Y. Zhang, J. Li, and A. Wu, Ultralight and superhydrophobic perfluorooctyltrimethoxysilane-modified biomass carbonaceous aerogel for oil-spill remediation, *Process Saf. Environ. Prot.*, 174(2021), p. 71
44. C. Wang, X. Cheng, K.H. Luo, K. Nandakumar, Z. Wang, M. Ni, X. Bi, J. Zhang, and C. Wang, A guided review of machine learning in the design and application for pore nanoarchitectonics of carbon materials, *Mater. Sci. Eng. R Rep.*, 165(2025), p. 101010
45. M. Chisaka, Review of carbon-support-free platinum and non-platinum catalysts for polymer electrolyte fuel cells: will they feature in future vehicles? *J. Mater. Chem. A*, 12(2024), p. 18636
46. S.G. Peera and S.W. Kim, Rare earth Ce/CeO_2 electrocatalysts: role of high electronic spin state of Ce and Ce^{3+}/Ce^{4+} redox couple on oxygen reduction reaction, *Nanomaterials*, 15(2025), p. 600.
47. J. Fang, K. Wang, P. Chen, X. Xu, C. Zhang, Y. Wu, Y. Yan, and Z. Zuo, Oxidation of soot by cerium dioxide synthesized under different hydrothermal conditions, *Molecules*, 30(2025), p. 1161.
48. T.Y. Ma, S. Dai, and S.Z. Qiao, Self-supported electrocatalysts for advanced energy conversion processes, *Mater. Today*, 19(2015), p. 265
49. S.G. Peera and C. Liu, Unconventional and scalable synthesis of non-precious metal electrocatalysts for practical proton exchange membrane and alkaline fuel cells: a solid-state coordination synthesis approach, *Coord. Chem. Rev.*, 463(2022), p. 214554.

50. A. Kumar, N. Goyal, S. Mathur, I.A. Bakhtiyarovich, Y. Zhao, M. Khalid, M. Ubaidullah, and A.M. Al-Enizi, Advances in coordination engineering of M–N–C single-atom catalysts for superior oxygen reduction performance, *Coord. Chem. Rev.*, 549(2025), p. 217244.
51. S. He and C. Sun, Fe-loaded S, N co-doped carbon catalyst for oxygen reduction reaction with enhanced electrocatalytic activity and durability, *Int. J. Miner. Metall. Mater.*, 33(2025), pp. 315.
52. R. Kumar, M. Mooste, I. Zekker, J. Kozlova, M. Käärik, M. Otsus, A. Treshchalov, J. Aruväli, J. Leis, A. Kikas, V. Kisand, K. Kukli, and K. Tammeveski, Mn–N–C material with high-density and accessible Mn–Nx sites emerging as an efficient oxygen reduction reaction electrocatalyst for AEMFCs, *J. Power Sources*, 667(2025), p. 239191.
53. N. Hussain, P. Parsai, A. Husain, and S.M. Mobin, Unraveling the recent advancement of single-atom catalysts derived from metal–organic frameworks for sustainable electrocatalysis, *ACS Sustain. Chem. Eng.*, 13(2025), p. 8829.
54. R. Li, X. Chen, Z. Bian, R. Yu, Y. Chen, J. Zhang, J. Wang, and X. Feng, Iridium-induced metal–organic framework honeycomb nanomaterials catalysis: a pathway to boosting hydrogen evolution reaction, *J. Alloys Compd.*, 1020(2025), p. 179345
55. Y. Duan, M. Chen, C. Wang, L. Gao, H. Luo, Y. Guan, Y. Zhou, J. Luo, R. Li, D. Wu, X. Tian, and Z. Miao, Recent advances in Fe-free M–N–C catalysts for oxygen reduction reaction, *ChemSusChem*, 18(2025), p. e202500430
56. S.R. Krishnan, D. Verstraete, and F. Aguey-Zinsou, Performance of non-precious metal electrocatalysts in proton-exchange membrane fuel cells: a review, *ChemElectroChem*, 11(2024), p. e202400299.
57. X. Hu, B. Yang, S. Ke, et al., Review and perspectives of carbon-supported platinum-based catalysts for proton exchange membrane fuel cells, *Energy Fuels*, 37(2023), p. 11532.
58. S. Xu, R. Peng, H. Sun, Z. Deng, Q. Wu, H. Jin, Y. Yang, and Z. Zhao, A time-efficient and safe method for scale-up synthesis of highly active Pt-based catalysts, *ACS Sustain. Chem. Eng.*, 13(2025), p. 4672.
59. Y. Nie, Z. Shi, B. Li, Q. Meyer, and C. Zhao, Engineering platinum-based alloy catalysts for oxygen reduction reaction in hydrogen fuel cells: a mini-review, *Energy Fuels*, 39(2025), p. 16049.
60. C. Wang, Z. Guo, Q. Shen, Y. Xu, C. Lin, X. Yang, C. Li, Y. Sun, and L. Hang, Recent advances in core–shell structured noble metal-based catalysts for electrocatalysis, *Rare Met.*, 44(2025), p. 2180.
61. W. Liu, A.-K. Herrmann, N.C. Bigall, P. Rodriguez, D. Wen, M. Oezaslan, T.J. Schmidt, N. Gaponik, A. Eychmüller, Noble metal aerogels—synthesis, characterization, and application as electrocatalysts, *Acc. Chem. Res.*, 48 (2015), p. 154
62. R. Du, X. Fan, X. Jin, R. Hübner, Y. Hu, A. Eychmüller, Emerging noble metal aerogels: state of the art and a look forward, *Matter*, 1 (2019), p. 39
63. S.G. Peera, M. Byun, Engineering gel-based precursors into advanced ORR catalysts for Zn–air batteries and fuel cells: insights into hydrogels, aerogels, xerogels, metal–organic gels, and metal aerogels, *Gels*, 11 (2025), p. 479.
64. R. Zhang, Y. Zhao, Preparation and electrocatalysis application of pure metallic aerogel: a review, *Catalysts*, 10 (2020), p. 1376.
65. W. Liu, P. Rodriguez, L. Borchardt, A. Foelske, J. Yuan, A. Herrmann, D. Geiger, Z. Zheng, S. Kaskel, N. Gaponik, R. Kötz, T.J. Schmidt, A. Eychmüller, Bimetallic aerogels: high-performance electrocatalysts for the oxygen reduction reaction, *Angew.*

Chem. Int. Ed., 52 (2013), p. 9849
66. N.C. Bigall, A. Herrmann, M. Vogel, M. Rose, P. Simon, W. Carrillo-Cabrera, D. Dorfs, S. Kaskel, N. Gaponik, A. Eychmüller, Hydrogels and aerogels from noble metal nanoparticles, *Angew. Chem. Int. Ed.*, 48 (2009), p. 9731.
67. A. Phadke, C. Zhang, B. Arman, et al., Rapid self-healing hydrogels, *Proc. Natl. Acad. Sci. U.S.A.*, 109 (2012), p. 4383
68. A.-K. Herrmann, P. Formanek, L. Borchardt, M. Klose, L. Giebeler, J. Eckert, S. Kaskel, N. Gaponik, A. Eychmüller, Multimetallic aerogels by template-free self-assembly of Au, Ag, Pt, and Pd nanoparticles, *Chem. Mater.*, 26 (2013), p. 1074
69. D. Wen, A. Eychmüller, 3D assembly of preformed colloidal nanoparticles into gels and aerogels: function-led design, *Chem. Commun.*, 53 (2017), p. 12608
70. H. Wang, Q. Fang, W. Gu, D. Du, Y. Lin, C. Zhu, Noble metal aerogels, *ACS Appl. Mater. Interfaces*, 12 (2020), p. 52234
71. C. Wang, W. Duan, L. Xing, Y. Xiahou, W. Du, H. Xia, Fabrication of Au aerogels with {110}-rich facets by size-dependent surface reconstruction for enzyme-free glucose detection, *J. Mater. Chem. B*, 7 (2019), p. 7588
72. W. Liu, A. Herrmann, D. Geiger, L. Borchardt, F. Simon, S. Kaskel, N. Gaponik, A. Eychmüller, High-performance electrocatalysis on palladium aerogels, *Angew. Chem. Int. Ed.*, 51 (2012), p. 5743
73. C. Wang, J. Herranz, R. Hübner, T.J. Schmidt, A. Eychmüller, Element distributions in bimetallic aerogels, *Acc. Chem. Res.*, 56 (2023), p. 237
74. G.W. Qin, J. Liu, T. Balaji, X. Xu, H. Matsunaga, Y. Hakuta, L. Zuo, P. Raveendran, A facile and template-free method to prepare mesoporous gold sponge and its pore size control, *J. Phys. Chem. C*, 112 (2008), p. 10352
75. X. Gao, R.J. Esteves, T.T.H. Luong, R. Jaini, I.U. Arachchige, Oxidation-induced self-assembly of Ag nanoshells into transparent and opaque Ag hydrogels and aerogels, *J. Am. Chem. Soc.*, 136 (2014), p. 7993
76. L. Jiao, W. Xu, H. Yan, Y. Wu, W. Gu, H. Li, D. Du, Y. Lin, C. Zhu, A dopamine-induced Au hydrogel nanozyme for enhanced biomimetic catalysis, *Chem. Commun.*, 55 (2019), p. 9865
77. R. Du, Y. Hu, R. Hübner, J.-O. Joswig, X. Fan, K. Schneider, A. Eychmüller, Specific ion effects directed noble metal aerogels: versatile manipulation for electrocatalysis and beyond, *Sci. Adv.*, 5 (2019), p. eaaw4590.
78. K.G.S. Ranmohotti, X. Gao, I.U. Arachchige, Salt-mediated self-assembly of metal nanoshells into monolithic aerogel frameworks, *Chem. Mater.*, 25 (2013), p. 3528
79. G. Picci, C. Caltagirone, A. Garau, V. Lippolis, J. Milia, J.W. Steed, Metal-based gels: synthesis, properties, and applications, *Coord. Chem. Rev.*, 492 (2023), p. 215225.
80. S.M. Jung, H.Y. Jung, M.S. Dresselhaus, Y.J. Jung, J. Kong, A facile route for 3D aerogels from nanostructured 1D and 2D materials, *Sci. Rep.*, 2 (2012), p. 849.
81. S.M. Jung, D.J. Preston, H.Y. Jung, Z. Deng, E.N. Wang, J. Kong, Porous Cu nanowire aerosponges from one-step assembly and their applications in heat dissipation, *Adv. Mater.*, 28 (2015), p. 1413
82. Y. Tang, K.L. Yeo, Y. Chen, L.W. Yap, W. Xiong, W. Cheng, Ultralow-density copper nanowire aerogel monoliths with tunable mechanical and electrical properties, *J. Mater. Chem. A*, 1 (2013), p. 6723
83. A. Freytag, S. Sánchez-Paradinas, S. Naskar, N. Wendt, M. Colombo, G. Pugliese, J. Poppe, C. Demirci, I. Kretschmer, D.W. Bahnemann, P. Behrens, N.C. Bigall, Versatile aerogel fabrication by freezing and subsequent freeze-drying of colloidal nanoparticle solutions, *Angew. Chem. Int. Ed.*, 55 (2015), p. 1200

84. R. Du, J. Joswig, R. Hübner, L. Zhou, W. Wei, Y. Hu, A. Eychmüller, Freeze–thaw-promoted fabrication of clean and hierarchically structured noble-metal aerogels for electrocatalysis and photoelectrocatalysis, *Angew. Chem. Int. Ed.*, 59 (2020), p. 8293
85. S. Naskar, A. Freytag, J. Deutsch, N. Wendt, P. Behrens, A. Köckritz, N.C. Bigall, Porous aerogels from shape-controlled metal nanoparticles directly from nonpolar colloidal solution, *Chem. Mater.*, 29 (2017), p. 9208
86. W. Liu, D. Haubold, B. Rutkowski, M. Oschatz, R. Hübner, M. Werheid, C. Ziegler, L. Sonntag, S. Liu, Z. Zheng, A.-K. Herrmann, D. Geiger, B. Terlan, T. Gemming, L. Borchardt, S. Kaskel, A. Czyrska-Filemonowicz, A. Eychmüller, Self-supporting hierarchical porous PtAg alloy nanotubular aerogels as highly active and durable electrocatalysts, *Chem. Mater.*, 28 (2016), p. 6477
87. B. Cai, R. Hübner, K. Sasaki, Y. Zhang, D. Su, C. Ziegler, M.B. Vukmirovic, B. Rellinghaus, R.R. Adzic, A. Eychmüller, Core–shell structuring of pure metallic aerogels towards highly efficient platinum utilization for the oxygen reduction reaction, *Angew. Chem. Int. Ed.*, 57 (2017), p. 2963
88. R. Du, J. Wang, Y. Wang, R. Hübner, X. Fan, I. Senkovska, Y. Hu, S. Kaskel, A. Eychmüller, Unveiling reductant chemistry in fabricating noble metal aerogels for superior oxygen evolution and ethanol oxidation, *Nat. Commun.*, 11 (2020), p. 1590.
89. M.Z. Yazdan-Abad, M. Noroozifar, A.R.M. Alam, H. Saravani, Palladium aerogel as a high-performance electrocatalyst for ethanol electro-oxidation in alkaline media, *J. Mater. Chem. A*, 5 (2017), p. 10244
90. M.Z. Yazdan-Abad, M. Noroozifar, A.S. Douk, A.R. Modarresi-Alam, H. Saravani, Shape engineering of palladium aerogels assembled by nanosheets to achieve a high-performance electrocatalyst, *Appl. Catal. B*, 250 (2019), p. 242
91. G. Ramanath, J. D'Arcy-Gall, T. Maddanimath, A.V. Ellis, P.G. Ganesan, R. Goswami, A. Kumar, K. Vijayamohanan, Templateless room-temperature assembly of nanowire networks from nanoparticles, *Langmuir*, 20 (2004), p. 5583
92. M.D. Ho, Y. Liu, D. Dong, Y. Zhao, W. Cheng, Fractal gold nanoframework for highly stretchable transparent strain-insensitive conductors, *Nano Lett.*, 18 (2018), p. 3593
93. C. Zhu, Q. Shi, S. Fu, J. Song, H. Xia, D. Du, Y. Lin, Efficient synthesis of MCu (M = Pd, Pt, and Au) aerogels with accelerated gelation kinetics and their high electrocatalytic activity, *Adv. Mater.*, 28 (2016), p. 8779
94. Q. Shi, C. Zhu, D. Du, C. Bi, H. Xia, S. Feng, M.H. Engelhard, Y. Lin, Kinetically controlled synthesis of AuPt bimetallic aerogels and their enhanced electrocatalytic performances, *J. Mater. Chem. A*, 5 (2017), p. 19626
95. X. Jiang, R. Du, R. Hübner, Y. Hu, A. Eychmüller, A roadmap for 3D metal aerogels: materials design and application attempts, *Matter*, 4 (2021), p. 54
96. S. Henning, L. Kühn, J. Herranz, J. Durst, T. Binninger, M. Nachtegaal, M. Werheid, W. Liu, M. Adam, S. Kaskel, A. Eychmüller, T.J. Schmidt, Pt–Ni aerogels as unsupported electrocatalysts for the oxygen reduction reaction, *J. Electrochem. Soc.*, 163 (2016), p. F998
97. S. Henning, H. Ishikawa, L. Kühn, J. Herranz, E. Müller, A. Eychmüller, T.J. Schmidt, Unsupported Pt–Ni aerogels with enhanced high-current performance and durability in fuel cell cathodes, *Angew. Chem.*, 129 (2017), p. 10847
98. S. Henning, J. Herranz, H. Ishikawa, B.J. Kim, D. Abbott, L. Kühn, A. Eychmüller, T.J. Schmidt, Durability of unsupported Pt–Ni aerogels in PEFC cathodes, *J. Electrochem. Soc.*, 164 (2017), p. F1136
99. K. Okaya, H. Yano, H. Uchida, M. Watanabe, Control of particle size of Pt and Pt alloy electrocatalysts supported on carbon black by the nanocapsule method, *ACS Appl.*

Mater. Interfaces, 2 (2010), p. 888
100. H. Ishikawa, S. Henning, J. Herranz, A. Eychmüller, M. Uchida, T.J. Schmidt, Tomographic analysis and modeling of polymer electrolyte fuel cell unsupported catalyst layers, *J. Electrochem. Soc.*, 165 (2018), p. F7
101. 101. F. Liu, Z. Gao, J. Su, L. Guo, Understanding the process of carbon corrosion and its impact on performance degradation during simulated start-stop operations for the proton exchange membrane fuel cell, *Electrochim. Acta*, 468 (2023), p. 143193.
102. S.J. Kim, S.J. Yoo, J.Y. Kim, S.K. Cho, H.S. Park, S.Y. Lee, B. Seo, J.H. Jang, K.H. Lim, H.-Y. Park, Impact of fuel starvation–induced anode carbon corrosion in proton exchange membrane fuel cells on the structure of the membrane electrode assembly and exhaust gas emissions: A quantitative case study, *J. Power Sources*, 615 (2024), p. 235032.
103. S. Henning, R. Shimizu, J. Herranz, L. Kühn, A. Eychmüller, M. Uchida, K. Kakinuma, T.J. Schmidt, Unsupported Pt_3Ni Aerogels as Corrosion Resistant PEFC Anode Catalysts under Gross Fuel Starvation Conditions *J. Electrochem. Soc.*, 165 (2018), p. F3001
104. 104. Y. Liu, O.C. Esan, Z. Pan, L. An, Machine learning for advanced energy materials, *Energy AI*, 3 (2021), p. 100049.
105. 105. M. Fikry, J. Herranz, S. Leisibach, P. Khavlyuk, A. Eychmüller, T.J. Schmidt, PEMFC-performance of unsupported Pt–Ni aerogel cathode catalyst layers under automotive-relevant operative conditions, *J. Electrochem. Soc.*, 170 (2023), p. 114524.
106. 106. M. Fikry, N. Weiß, M. Bozzetti, S. Ünsal, M. Georgi, P. Khavlyuk, J. Herranz, V. Tileli, A. Eychmüller, T.J. Schmidt, Up-scaled preparation of Pt–Ni aerogel catalyst layers for polymer electrolyte fuel cell cathodes, *ACS Appl. Energy Mater.*, 7 (2024), p. 896
107. 107. S. Członka, M.F. Bertino, J. Kośny, N. Shukla, Freeze-drying method as a new approach to the synthesis of polyurea aerogels from isocyanate and water, *J. Sol-Gel Sci. Technol.*, 87 (2018), p. 685
108. 108. X. Wang, Z. Li, Y. Qu, T. Yuan, W. Wang, Y. Wu, Y. Li, Review of metal catalysts for oxygen reduction reaction: From nanoscale engineering to atomic design, *Chem*, 5 (2019), p. 1486
109. X. Wang, M. Vara, M. Luo, H. Huang, A. Ruditskiy, J. Park, S. Bao, J. Liu, J. Howe, M. Chi, Z. Xie, Y. Xia, Pd@Pt core–shell concave decahedra: A class of catalysts for the oxygen reduction reaction with enhanced activity and durability, *J. Am. Chem. Soc.*, 137 (2015), p. 15036–15042.
110. 110. R. Du, W. Jin, R. Hübner, L. Zhou, Y. Hu, A. Eychmüller, Engineering multimetallic aerogels for pH-universal HER and ORR electrocatalysis, *Adv. Energy Mater.*, 10 (2020), p. 1903857.
111. T. López-León, M.J. Santander-Ortega, J.L. Ortega-Vinuesa, D. Bastos-González, Hofmeister effects in colloidal systems: Influence of the surface nature, *J. Phys. Chem. C*, 112 (2008), p. 16060
112. Z. Chen, Y. Liao, S. Chen, Facile synthesis of platinum–copper aerogels for the oxygen reduction reaction, *Energy Mater.*, 2 (2022), p. 200033.
113. A.S. Pavlets, A.A. Alekseenko, A.V. Nikolskiy, A.T. Kozakov, O.I. Safronenko, I.V. Pankov, V.E. Guterman, Effect of the PtCu/C electrocatalysts initial composition on their activity in the de-alloyed state in the oxygen reduction reaction, *Int. J. Hydrogen Energy*, 47 (2022), p. 30460
114. Y. Zheng, A.S. Petersen, H. Wan, R. Hübner, J. Zhang, J. Wang, H. Qi, Y. Ye, C. Liang, J. Yang, Z. Cui, Y. Meng, Z. Zheng, J. Rossmeisl, W. Liu, Scalable and

controllable synthesis of Pt–Ni bunched-nanocages aerogels as efficient electrocatalysts for oxygen reduction reaction, *Adv. Energy Mater.*, 13 (2023), p. 2204257.
115. Y. Qin, W. Zhang, K. Guo, X. Liu, J. Liu, X. Liang, X. Wang, D. Gao, L. Gan, Y. Zhu, Z. Zhang, W. Hu, Fine-tuning intrinsic strain in penta-twinned Pt–Cu–Mn nanoframes boosts oxygen reduction catalysis, *Adv. Funct. Mater.*, 30 (2020), p. 1910107.
116. S. Luo, Y. Luo, H. Wu, M. Li, L. Yan, K. Jiang, L. Liu, Q. Li, S. Fan, J. Wang, Self-assembly of 3D carbon nanotube sponges: A simple and controllable way to build macroscopic and ultralight porous architectures, *Adv. Mater.*, 29 (2016), p. 1603549.
117. C. Chen, Y. Kang, Z. Huo, Z. Zhu, W. Huang, H.L. Xin, J.D. Snyder, D. Li, J.A. Herron, M. Mavrikakis, M. Chi, K.L. More, Y. Li, N.M. Markovic, G.A. Somorjai, P. Yang, V.R. Stamenkovic, Highly crystalline multimetallic nanoframes with three-dimensional electrocatalytic surfaces, *Science*, 343 (2014), p. 1339
118. Q. Shi, C. Zhu, H. Zhong, D. Su, N. Li, M.H. Engelhard, H. Xia, Q. Zhang, S. Feng, S.P. Beckman, D. Du, Y. Lin, Nanovoid-incorporated Ir–Cu metallic aerogels for oxygen evolution reaction catalysis, *ACS Energy Lett.*, 3 (2018), p. 2038
119. C. Zhu, Q. Shi, S. Fu, J. Song, D. Du, D. Su, M.H. Engelhard, Y. Lin, Core–shell PdPb@Pd aerogels with multiply twinned intermetallic nanostructures: Facile synthesis with accelerated gelation kinetics and enhanced electrocatalytic properties, *J. Mater. Chem. A*, 6 (2018), p. 7517
120. Q. Liu, B. Yu, X. Liao, Y. Zhao, Facet-dependent oxygen reduction reaction activity on the surfaces of Co_3O_4, *Energy Environ. Mater.*, 4 (2020), p. 407
121. 121. W. Duan, P. Zhang, Y. Xiahou, Y. Song, C. Bi, J. Zhan, W. Du, L. Huang, H. Möhwald, H. Xia, Regulating surface facets of metallic aerogel electrocatalysts by size-dependent localized Ostwald ripening, *ACS Appl. Mater. Interfaces*, 10 (2018), p. 23081
122. L. Kühn, A. Herrmann, B. Rutkowski, M. Oezaslan, M. Nachtegaal, M. Klose, L. Giebeler, N. Gaponik, J. Eckert, T.J. Schmidt, A. Czyrska-Filemonowicz, A. Eychmüller, Alloying behavior of self-assembled noble metal nanoparticles, *Chem. Eur. J.*, 22 (2016), p. 13446
123. Q. Shi, C. Zhu, M. Tian, D. Su, M. Fu, M.H. Engelhard, I. Chowdhury, S. Feng, D. Du, Y. Lin, Ultrafine Pd ensembles anchored Au_2Cu aerogels boost ethanol electrooxidation, *Nano Energy*, 53 (2018), p. 206
124. Q. Shi, W. Zhu, H. Zhong, C. Zhu, H. Tian, J. Li, M. Xu, D. Su, X. Li, D. Liu, B.Z. Xu, S.P. Beckman, D. Du, Y. Lin, Highly dispersed platinum atoms on the surface of Au–Cu metallic aerogels for enabling H_2O_2 production, *ACS Appl. Energy Mater.*, 2 (2019), p. 7722
125. H. Fu, H. Huang, Y. Chen, K. Jiang, F. Lai, C. Chen, Z. Zhang, H. Li, N. Zhang, T. Liu, Lattice-strained metallic aerogels as efficient and anti-poisoning electrocatalysts for oxygen reduction reaction, *ChemSusChem*, 17 (2023), p. e202301221.
126. Z. Hou, C. Cui, Y. Li, Y. Gao, D. Zhu, Y. Gu, G. Pan, Y. Zhu, T. Zhang, Lattice-strain engineering for heterogeneous electrocatalytic oxygen evolution reaction, *Adv. Mater.*, 35 (2023), p. 2209876.
127. L. Bu, N. Zhang, S. Guo, X. Zhang, J. Li, J. Yao, T. Wu, G. Lu, J.-Y. Ma, D. Su, X. Huang, Biaxially strained PtPb/Pt core–shell nanoplate boosts oxygen reduction catalysis, *Science*, 354 (2016), p. 1410
128. D. Liu, Q. Zeng, C. Hu, H. Liu, D. Chen, Y. Han, L. Xu, J. Yang, Core–shell CuPd@NiPd nanoparticles: Coupling lateral strain with electronic interaction toward high-efficiency electrocatalysis, *ACS Catal.*, 12 (2022), p 9092

129. K. Wang, M. Wang, Q. Lei, T. Zhou, X. Liu, Z. Cao, Z. Jiang, J. He, Strain effect of PtCu alloy aerogel nanocatalysts on oxygen reduction reaction enhancement, *Mol. Catal.*, 580 (2025), p. 115121.
130. S. Aralekallu, V. Singh, M–N–C-based non-precious metal catalyst materials for electrocatalytic ORR applications, *Fuel*, 404 (2025), p. 136163.
131. Y. Lin, W. Li, Z. Wang, Y. Zheng, Y. Zhang, X. Fu, Current advances and performance enhancement of single atom M–N–C catalysts for PEMFCs, *Front. Energy* 19 (2025), p. 642
132. T. Song, H. Xue, J. Sun, N. Guo, J. Sun, Q. Wang, Solvent assistance induced surface N-modification of PtCu aerogels and their enhanced electrocatalytic properties, *Chem. Commun.* 57 (2021), p. 7140
133. X. Xiang, X. Li, Z. Huang, T. Gao, H. Yuan, D. Xiao, Sphere- and flake-structured Cu, N co-doped carbon catalyst designed by a template-free method for robust oxygen reduction reaction, *ChemElectroChem* 6 (2019), p. 1078
134. J. Liu, W. Li, R. Cheng, Q. Wu, J. Zhao, D. He, S. Mu, Stabilizing Pt nanocrystals encapsulated in N-doped carbon as double-active sites for catalyzing oxygen reduction reaction, *Langmuir* 35 (2019), p. 2580
135. Y. Zhou, L. Sheng, L. Chen, W. Zhao, W. Zhang, J. Yang, Metal and ligand modification modulates the electrocatalytic HER, OER, and ORR activity of 2D conductive metal–organic frameworks, *Nano Res.* 17 (2024), p. 7984
136. P. Liu, R. Qin, G. Fu, N. Zheng, Surface coordination chemistry of metal nanomaterials, *J. Am. Chem. Soc.* 139 (2017), p. 2122
137. X. Fan, S. Zerebecki, R. Du, R. Hübner, G. Marzum, G. Jiang, Y. Hu, S. Barcikowski, S. Reichenberger, A. Eychmüller, Promoting the electrocatalytic performance of noble metal aerogels by ligand-directed modulation, *Angew. Chem. Int. Ed.* 59 (2020), p. 5706
138. D. Wen, W. Liu, D. Haubold, C. Zhu, M. Oschatz, M. Holzschuh, A. Wolf, F. Simon, S. Kaskel, A. Eychmüller, Gold aerogels: three-dimensional assembly of nanoparticles and their use as electrocatalytic interfaces, *ACS Nano* 10 (2016), p. 2559
139. H. Yuan, X. Wan, J. Ye, T. Ma, F. Ma, J. Gao, W. Gao, D. Wen, Molecular engineering of noble metal aerogels boosting electrocatalytic oxygen reduction, *Adv. Funct. Mater.* 33 (2023), p. 2302561.
140. R.W. Seidel, I.M. Oppel, 1D and 2D solid-state metallosupramolecular arrays of freebase 5,10,15,20-tetra(4-pyridyl)porphyrin peripherally linked by zinc and manganese ions, *Struct. Chem.* 20 (2009), p. 121
141. W. Auwärter, F. Klappenberger, A. Weber-Bargioni, A. Schiffrin, T. Strunskus, C. Wöll, Y. Pennec, A. Riemann, J.V. Barth, Conformational adaptation and selective adatom capturing of tetrapyridyl-porphyrin molecules on a Cu(111) surface, *J. Am. Chem. Soc.* 129 (2007), p. 11279
142. Z. Liang, H.-Y. Wang, H. Zheng, W. Zhang, R. Cao, Porphyrin-based frameworks for oxygen electrocatalysis and catalytic reduction of carbon dioxide, *Chem. Soc. Rev.* 50 (2021), p. 2540
143. R. Chen, H. Li, D. Chu, G. Wang, Unraveling oxygen reduction reaction mechanisms on carbon-supported Fe-phthalocyanine and Co-phthalocyanine catalysts in alkaline solutions, *J. Phys. Chem. C* 113 (2009), p. 20689
144. H. Yuan, W. Gao, X. Wan, J. Ye, F. Ma, D. Wen, Surface engineering of Pt aerogels by metal phthalocyanine to enhance the electrocatalytic property for oxygen reduction reaction, *Mater. Today Energy* 37 (2023), p. 101379.
145. H. Yuan, W. Gao, X. Wan, J. Ye, D. Wen, Tuning the surface electronic structure of noble metal aerogels to promote the electrocatalytic oxygen reduction, *J. Energy Chem.*

89 (2023), p. 557

146. A. Avid, J.L. Ochoa, Y. Huang, Y. Liu, P. Atanassov, I.V. Zenyuk, Revealing the role of ionic liquids in promoting fuel cell catalyst reactivity and durability, *Nat. Commun.* 13 (2022), p. 6349.
147. H. Yuan, W. Gao, J. Ye, T. Ma, F. Ma, D. Wen, Surface hydrophobicity engineering of Pt-based noble metal aerogels by ionic liquids toward enhanced electrocatalytic oxygen reduction, *ACS Appl. Mater. Interfaces* 15 (2023), p. 21143
148. J. Snyder, T. Fujita, M.W. Chen, J. Erlebacher, Oxygen reduction in nanoporous metal–ionic liquid composite electrocatalysts, *Nat. Mater.* 9 (2010), p. 904
149. Y. Zhang, X. Mu, Z. Liu, H. Zhao, Z. Zhuang, Y. Zhang, S. Mu, S. Liu, D. Wang, Z. Dai, Twin-distortion-modulated ultra-low coordination PtRuNi–Ox catalyst for enhanced hydrogen production from chemical wastewater, *Nat. Commun.* 15 (2024), p. 10149.
150. L. Bu, B. Huang, Y. Zhu, F. Ning, X. Zhou, X. Huang, Highly distorted platinum nanorods for high-efficiency fuel cell catalysis, *CCS Chem.* 2 (2020), p. 401
151. X. Zhang, Y. Yang, Y. Liu, Z. Jia, Q. Wang, L. Sun, L. Zhang, J.J. Kruzic, J. Lu, B. Shen, Defect engineering of a high-entropy metallic glass surface for high-performance overall water splitting at ampere-level current densities, *Adv. Mater.* 35 (2023), p. 2303439.
152. H. Wang, Q. He, X. Gao, Y. Shang, W. Zhu, W. Zhao, Z. Chen, H. Gong, Y. Yang, Multifunctional high-entropy alloys enabled by severe lattice distortion, *Adv. Mater.* 36 (2024), p. 2305453.
153. G. Yan, T. Wang, H. Xue, M. Zhang, Z. Xu, F. Chen, W. Yu, Ultrathin two-dimensional medium-entropy alloy as a highly efficient and stable electrocatalyst for oxygen evolution reaction, *Int. J. Miner. Metall. Mater.* 32 (2025), p. 2767
154. J. Xia, J. Zhang, M. Xiu, B. Zhang, Z. Zhou, Y. Lu, Y. Huang, J. Wu, Ultrafast laser synthesis of sub-10 nm FeCoNiMnCr high-entropy alloy nanoparticles for enhanced oxygen evolution catalysis, *Int. J. Miner. Metall. Mater.* 32 (2025), p. 2756
155. X. Zhu, W. Huang, Y. Lou, Z. Yao, H. Ying, M. Dong, L. Tan, J. Zeng, H. Ji, H. Zhu, S. Lan, Ultrafast joule-heating synthesis of FeCoMnCuAl high-entropy-alloy nanoparticles as efficient OER electrocatalysts, *Prog. Nat. Sci. Mater. Int.* 34 (2024), p. 880
156. G. Han, M. Li, H. Liu, W. Zhang, L. He, F. Tian, Y. Liu, Y. Yu, W. Yang, S. Guo, Short-range diffusion enables general synthesis of medium-entropy alloy aerogels, *Adv. Mater.* 34 (2022), p. 2202943.
157. J. Wang, J. Jiang, P.K. Liaw, Y. Zhang, Properties and performances of high-entropy materials in batteries, *Int. J. Miner. Metall. Mater.* 32 (2025), p. 2786
158. G. Wang, X. Li, X. Yang, L. Liu, Y. Cai, Y. Wu, S. Wang, H. Li, Y. Zhou, Y. Wang, Y. Zhou, Metal-based aerogel catalysts for electrocatalytic CO_2 reduction, *Chem. Eur. J.* 28 (2022), p. 202201834.
159. H. Li, F. Yang, G. Wang, L. Guan, F. Lai, N. Zhang, T. Liu, Highly distorted high-entropy alloy aerogels for high-efficiency hydrogen oxidation reaction, *ACS Nano* 19 (2025), p. 14434
160. J. Wang, F. Chen, Y. Jin, R.L. Johnston, Gold–copper aerogels with intriguing surface electronic modulation as highly active and stable electrocatalysts for oxygen reduction and borohydride oxidation, *ChemSusChem* 11 (2018), p. 1354
161. X. Wu, C. Ni, J. Man, X. Shen, S. Cui, X. Chen, A strategy to promote the ORR electrocatalytic activity by engineering a bunched three-dimensional Pd–Cu alloy

aerogel, *Chem. Eng. J.* 454 (2023), p. 140293.

162. X. Wu, L. Liu, K. Yuan, Y. Shao, X. Shen, S. Cui, X. Chen, Modulating electronic structure and atomic insights into a hierarchically porous PdCuFe trimetallic alloy aerogel for efficient oxygen reduction, *Small* 20 (2024), p. 2307243.
163. H. Fu, J. Wang, Y. Chen, H. Huang, Y. Wang, H. Li, F. Lai, L. Zhang, N. Zhang, J. Chen, T. Liu, Pd_3Pb bimetallic aerogels for anti-poisoned oxygen reduction reaction, *Chem. Eng. J.* 470 (2023), p. 144255.
164. K. Dong, Y. Zhang, Z. Zheng, X. Yang, Q. Yuan, Au-enabled PdAu aerogel efficient catalysts for oxygen reduction and C_2 alcohol oxidation, *Int. J. Hydrogen Energy* 78 (2024), p. 443
165. C. Wang, W. Wei, M. Georgi, R. Hübner, C. Steinbach, Y. Bräuniger, S. Schwarz, S. Kaskel, A. Eychmüller, Direct synthesis of Pd^{2+}-rich palladene aerogels as bifunctional electrocatalysts for formic acid oxidation and oxygen reduction reactions, *ChemElectroChem* 11 (2024), p. 202400060.
166. K. Yuan, Y. Zheng, Y. Zhao, L. Liu, A. Altaf, Y. Chen, A. Wang, X. Wu, S. Cui, Bimetallic self-supported AuCu alloy aerogel with abundant diffusion channels for regulating oxygen reduction reaction by electronic structure modulation for zinc–air batteries, *Chem. Eng. J.* 505 (2025), p. 159930.
167. Y. Bai, W. Hao, A. Altaf, J. Lu, L. Liu, C. Zhu, X. Gu, X. Wu, X. Shen, S. Cui, X. Chen, Construction of PdCu alloy decorated on N-doped carbon aerogel as a highly active electrocatalyst for enhanced oxygen reduction reaction, *Gels* 11 (2025), p. 166.